Review of high-power microwave source research

Steven H. Gold
Beam Physics Branch, Plasma Physics Division, Naval Research Laboratory, Washington, DC 20375-5346

Gregory S. Nusinovich
Institute for Plasma Research, University of Maryland, College Park, Maryland 20742

(Received 18 March 1997; accepted for publication 7 August 1997)

This article reviews the state-of-the-art in high-power microwave source research. It begins with a discussion of the concepts involved in coherent microwave generation. The main varieties of microwave tubes are classified into three groups, according to the fundamental radiation mechanism involved: Cherenkov, transition, or bremsstrahlung radiation. This is followed by a brief discussion of some of the technical fundamentals of high-power microwave sources, including power supplies and electron guns. Finally, the history and recent developments of both high-peak power and high-average power sources are reviewed in the context of four main areas of application: (1) plasma resonance heating and current drive; (2) rf acceleration of charged particles; (3) radar and communications systems; and (4) high-peak power sources for weapons-effect simulation and exploratory development. © *1997 American Institute of Physics.* [S0034-6748(97)01511-6]

I. INTRODUCTION

One of the classic applications of electron beams is the generation of coherent electromagnetic radiation. The development of sources of radiation in the microwave portion of the electromagnetic spectrum, which extends from approximately 300 MHz to 300 GHz, began many years ago. However, an impressive increase in the power and operating frequency of these sources has taken place in the last few decades, due to progress in a new branch of physics that can be called ''relativistic high-frequency electronics.'' The term ''relativistic'' refers first to the use of high-voltage electron beams with velocities close to the speed of light, which can have very high current densities, and second to the appearance of new microwave sources based on specific relativistic effects. As will be shown below, some of these relativistic effects can be important even at low voltages, when electron velocities are much smaller than the speed of light. The progress results from three main developments: the use of higher currents and voltages in conjunction with conventional microwave device concepts, such as klystrons and magnetrons; the development of new device concepts that rely specifically on these very high currents, such as vircators; and the research into new fast-wave devices, such as gyrotrons and free-electron lasers, that make direct use of relativistic effects, and extrapolate to higher powers at shorter wavelengths than conventional devices.

This article is intended to provide an introduction to some of the concepts and technologies involved in the development of high-power microwave (HPM) sources and to describe some of the recent progress in the field. We will include in our consideration, microwave sources operating in both the high-peak power (short-pulse, low-repetition rate) and high-average power (long-pulse, high-repetition rate or continuous-wave) regimes, even though the instantaneous power levels in these two regimes are quite different. Moreover, high power for a broadband amplifier tube can be very different than high power for a long-pulse oscillator. Our common thread is to discuss current research and recent advances in vacuum (and some plasma-filled) microwave devices, and to define high power in the context of the particular type of device under consideration. The article is organized as follows: Section II describes the physics of sources of coherent microwave radiation; Sec. III presents some technical fundamentals of HPM devices; and Sec. IV discusses the state-of-the-art in the development of HPM sources. In order to organize Sec. IV, we have divided microwave source research into four main areas, based on the existing or potential applications of these sources:

(1) resonance heating and current drive of thermonuclear fusion plasmas (high-average power oscillators);

(2) rf acceleration in high-energy linear colliders (high-power, narrow-band amplifiers, both millimeter and centimeter wave);

(3) radar and communications systems (mostly moderate-power, broad-bandwidth millimeter-wave amplifiers);

(4) high-peak-power sources for weapons-effects simulators and exploratory research.

Finally, we present a summary in Sec. V.

II. SOURCE VARIETIES AND SOURCE PHYSICS: CHERENKOV, TRANSITION, AND BREMSSTRAHLUNG RADIATION

Microwave tubes use electrons to generate coherent electromagnetic radiation. Coherent radiation is produced when electrons that are initially uncorrelated, and produce spontaneous emission with random phase, are gathered into microbunches that radiate in phase. There are three basic kinds of electromagnetic radiation by charged particles: (1) Cherenkov or Smith–Purcell radiation of slow waves propa-

gating with velocities less than the speed of light in vacuum, (2) transition radiation, and (3) bremsstrahlung. (This subject is treated at greater length in Ref. 1.)

A. Cherenkov radiation

Cherenkov radiation occurs when electrons move in a medium with a refractive index $n>1$, and the electron velocity, v, is greater than the phase velocity of the electromagnetic waves, $v_{ph}=c/n$, where c is the vacuum speed of light. This radiation process can occur only when the refractive index is large enough: $n>c/v$.

Slow waves (i.e., waves with $v_{ph}<c$) may also exist in periodic structures, where, in accordance with Floquet's theorem, an electromagnetic wave can be represented as the superposition of spatial harmonics $E=e^{-i\omega t}\sum_{l=-\infty}^{+\infty}A_l e^{ik_{zl}z}$ with axial wave numbers $k_{zl}=k_{z0}+2\pi l/d$. Here, ω is the angular frequency of the radiation, d is the structure period, l is the harmonic number, k_{z0} is the wave number of the zeroth-order spatial harmonic ($-\pi/d<k_{z0}<\pi/d$), and the ratio of the coefficients A_l is determined by the shape of the structure. Electromagnetic radiation from electrons in a periodic slow-wave structure is known as Smith–Purcell radiation. One can consider a spatial harmonic with phase velocity $v_{ph}=\omega/k_{zl}<c$ as a slow wave propagating in a medium with a refractive index $n=ck_{zl}/\omega$. This allows one to understand Smith–Purcell radiation as a kind of Cherenkov radiation. Note that the transverse wave number of slow waves is imaginary:

$$k_{\perp l}^2=\left(\frac{\omega}{c}\right)^2-k_{zl}^2<0.$$

This means that the field of the corresponding spatial harmonic is localized near the structure wall, and, therefore, that electrons should also propagate close to the wall to couple to this wave.

Well-known microwave tubes based on Cherenkov/Smith–Purcell radiation include traveling-wave tubes (TWTs) and backward-wave oscillators (BWOs). The principle of their operation is illustrated in Fig. 1. Figure 1(a) shows a schematic of a traveling-wave tube, in which an electron beam guided by an external magnetic field amplifies an injected electromagnetic wave in a periodic rippled-wall structure. Figure 1(b) shows a similar schematic for a backward-wave oscillator. Figure 1(c) shows the corresponding dispersion diagrams, i.e., the dependence of the wave frequency on its axial wave number, in a slow-wave structure with period d. (The dispersion curve is shown for the first passband of the TM_{01} mode; dispersion curves for higher passbands of the TM_{01} mode and those for higher-order modes are located at higher frequencies.) The dashed line in Fig. 1(c) is the light line, $\omega=k_z c$, which is the boundary between regions of fast ($v_{ph}=\omega/k_z>c$) and slow ($v_{ph}<c$) waves. The passband, i.e., the difference between the minimum frequency (the cutoff frequency at points $k_z=0$, $2\pi/d,\ldots$) and the maximum frequency (at π points $k_z=\pi/d$, $3\pi/d,\ldots$), depends on the height of the wall ripples.[2] The operating point is determined by the intersection of the dispersion curve with the beam line $\omega=k_z v_z$, corresponding to the condition of Cherenkov synchronism, $v_{ph}=v_z$ [see Fig. 1(c)]. [This beam line approximates the dispersion curves for the fast and slow space-charge waves, which satisfy the dispersion relation $\omega=k_z v_z\pm\omega_b$, where ω_b is the beam plasma frequency. The interaction takes place with the slow space-charge wave, $\omega=k_z v_z-\omega_b$, a negative-energy wave whose growth decreases the kinetic energy of the beam (see Ref. 3).] TWTs operate in portions of the dispersion curve where the group velocity of the slow wave, $v_{gr}=d\omega/dk_z$, is positive (e.g., for the curve shown, $\omega/c<k_z<\pi/d$, $2\pi/d<k_z<3\pi/d$, etc.), and amplify forward waves, which propagate in the same direction as the electron beam. For the TWT interaction shown in Fig. 1(c), the electrons interact with the zeroth-order spatial harmonic of the forward wave. BWOs operate in regions where the group velocity is negative ($\pi/d<k_z<2\pi/d$, etc.), and amplify backward waves, which propagate in the opposite direction as the electron beam, thus providing an internal feedback mechanism. For the BWO interaction shown in Fig. 1(c), the electrons interact with the first spatial harmonic of the backward wave, and for the BWO illustrated in Fig. 1(b), the backward wave reflects from the cutoff waveguide at the electron beam entrance as a forward wave, and emerges from the tube at the same end as the electron beam. Since this forward wave does not satisfy the condition of Cherenkov synchronism, it does not interact synchronously with the electron beam. [In some cases, the asynchronous interaction between electrons and the forward wave can also be important (see Ref. 4 and references therein.)] By changing the operating voltage (electron velocity) and/or the structure period, one can, in prin-

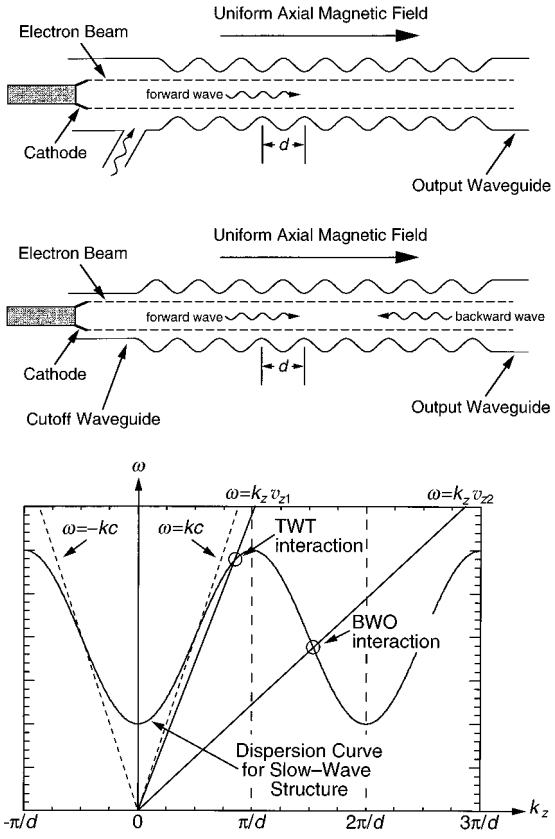

FIG. 1. (a) Schematic of a TWT; (b) schematic of a BWO; (c) dispersion diagrams for Cherenkov devices.

ciple, move the point of intersection of the beam line with the dispersion curve to any point below the light line.

Let us show how the parameters of the interaction region in Cherenkov devices scale with the electron energy. First, note that the formation of a compact electron bunch requires that the modulation of electron velocities, Δv_z, due to the interaction with an electromagnetic (EM) wave, should cause a displacement of particles of order $\lambda/2$ after they have transited the interaction length L, where λ is the free-space wavelength. The corresponding condition can be written as

$$\Delta v_z \frac{L}{v_{z0}} \sim \frac{\lambda}{2}. \tag{1}$$

Using the relativistic formula $\gamma = 1/\sqrt{1-(v/c)^2}$, where γ is the electron energy normalized to m_0c^2, v is the total electron velocity, and m_0 is the electron rest mass, and assuming that the transverse velocity $v_\perp = 0$, the changes in electron velocity and energy are related as

$$\frac{\Delta v_z}{v_{z0}} = \frac{1}{(\gamma_0^2 - 1)} \frac{\Delta \gamma}{\gamma_0}. \tag{2}$$

Here, $\gamma_0 = 1 + eV_b/m_0c^2$, where V_b is the beam voltage. Equation (2) shows that the velocities of initially highly relativistic electrons can remain close to c, even after a significant fraction of their kinetic energy is extracted. This fact is favorable for maintaining synchronism between the wave and the decelerating electron.

Using Eq. (2), one can rewrite Eq. (1) as

$$\frac{2}{\gamma_0^2 - 1} \frac{\Delta \gamma}{\gamma_0} \sim \frac{\lambda}{L}. \tag{3}$$

For deep deceleration ($\Delta\gamma \sim \gamma_0 - 1$), Eq. (3) is reduced to

$$\frac{L}{\lambda} \sim \frac{\gamma_0(\gamma_0 + 1)}{2}. \tag{4}$$

Equation (4) shows that at low voltages ($\gamma_0 - 1 \ll 1$), the interaction length required for the bunch formation does not depend on the initial electron energy, while at high voltages ($\gamma_0 \gg 1$), it scales as γ_0^2.

The work done by the synchronous harmonic of an EM wave on an electron after a distance L is equal to the change in electron energy. To simplify, we assume that the wave amplitude A is constant. Then A obeys the equation

$$AL = \Delta\gamma \frac{m_0c^2}{e}. \tag{5}$$

For deep deceleration, combining Eqs. (4) and (5) gives

$$A \sim 2 \frac{m_0c^2}{e\lambda} \frac{\gamma_0 - 1}{\gamma_0(\gamma_0 + 1)}. \tag{6}$$

Equation (6) shows that the amplitude of the synchronous harmonic should be proportional to V_b at low voltages, and proportional to γ_0^{-1} at high voltages.

In a BWO, the radiated microwave power is proportional to A_0^2, where A_0 is the amplitude of the zeroth-order spatial harmonic, and accordingly A_0 should be proportional to $P_b^{1/2}$, where $P_b = I_bV_b$. However, the amplitude of the synchronous first-order spatial harmonic, A_1, should be set according to Eq. (6), which scales inversely with γ_0 at high voltages. To satisfy both of these constraints requires that

$$\frac{A_1}{A_0} \propto \frac{1}{\gamma_0\sqrt{P_b}}.$$

The ratio A_1/A_0 can be controlled by proper design of the slow-wave structure, since the amplitude of the higher-order spatial harmonics is proportional to the height of the ripples. In some cases, as will be shown below, the limiting current for high-voltage electron beams scales as $I_b \sim \gamma_0$, so that

$$\frac{A_1}{A_0} \propto \frac{1}{\gamma_0^2}.$$

The fact that the amplitude A_1 of the slow wave localized near the wall is inversely proportional to a power of the electron energy is important in reducing the possibility of rf breakdown of the structure.

It is noteworthy that not only the axial wave number corresponds to the condition of Cherenkov synchronism, $k_z = \omega/v_{z0}$, but also the transverse wave number of the synchronous wave scales with the electron energy:

$$k_\perp^2 = \left(\frac{\omega}{c}\right)^2 - k_z^2 = \left(\frac{\omega}{c}\right)^2 (1 - \beta_{z0}^{-2}).$$

This equation shows that the transverse distance, $L_\perp$, within which the field of the synchronous slow-wave spatial harmonic is localized near the structure walls, scales with the electron energy as

$$L_\perp \sim (\gamma_0^2 - 1)^{1/2}\lambda. \tag{7}$$

Equation (7) allows a better clearance between the electrons and structure walls for relativistic Cherenkov devices than for their weakly relativistic counterparts.

Cross-field devices such as magnetrons differ from linear-beam devices such as TWTs and BWOs in that they convert the potential energy of electrons into microwave power as the electrons drift from the cathode to the anode. Nevertheless, they can be treated as Cherenkov devices because the electron drift velocity in the crossed external electric and magnetic fields, v_{dr}, is close to the phase velocity of a slow electromagnetic wave [see Fig. 2(a)]. Hence the condition for Cherenkov synchronism between the wave propagation and the electron motion is fulfilled. (For cylindrical magnetrons, this is known as the Buneman–Hartree resonance condition.) Note that when the beam power increases, the anode surface can deteriorate in the area of the beam energy deposition. For this reason, some short-wavelength relativistic magnetrons employ a microwave structure with an open output end [see Fig. 2(b)], through which high-power microwaves can propagate without breakdown, and through which the electron beam can move to a larger area collector.

B. Transition radiation

Transition radiation occurs when electrons pass through a border between two media with different refractive indices, or through some perturbation in the medium such as conducting grids or plates. In radio-frequency tubes, these per-

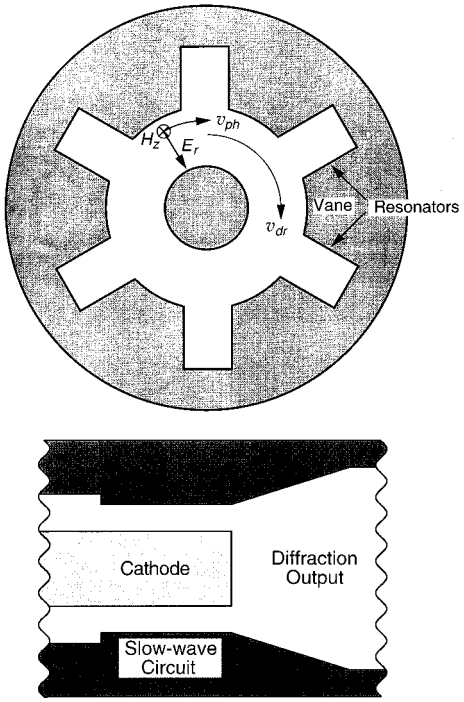

FIG. 2. (a) Schematic diagram of a magnetron; (b) diagram of a magnetron with diffraction output coupling.

turbations are grids. In microwave tubes such as klystrons, they are short-gap cavities, within which the microwave fields are localized.

Klystrons are the most common type of device based on coherent transition radiation from electrons. A typical klystron amplifier (see Fig. 3) consists of one or more cavities, separated by drift spaces, that are used to form electron bunches from an initially uniform electron flow by modulating the electron velocity using the axial electric fields of a transverse magnetic (TM) mode, followed by an output cavity that produces coherent radiation by decelerating the electron bunches. The basic limitations on power as a function of frequency are determined by the output cavity, which must extract a significant fraction of the electron kinetic energy in a length limited by the electron transit time. The transit angle $\theta=\omega L/v_z$ cannot exceed π in order to maintain a favorable rf phase in the cavity gap.

In the nonrelativistic limit, the requirement to extract all

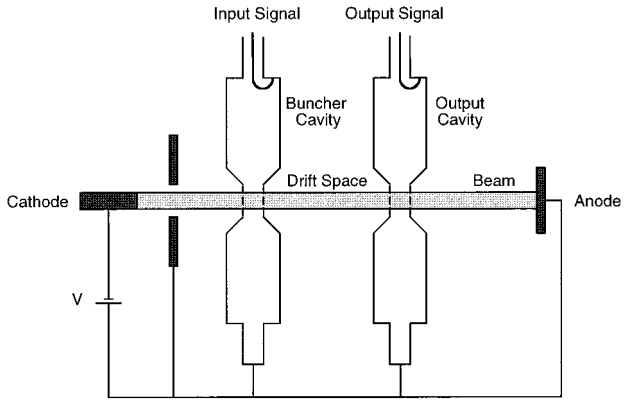

FIG. 3. Schematic diagram of a two-cavity klystron amplifier.

of the kinetic energy from an electron in 1/2 rf period has an exact solution that is easily derived. It requires a cavity gap of length

$$d=\frac{\pi}{\omega}\sqrt{\frac{eV_b}{2m_0}}, \tag{8}$$

where eV_b is the electron energy, with a peak gap voltage $V_{\text{gap}}=\pi V_b/2$. The peak rf electric field is therefore

$$E_z=\omega\sqrt{\frac{m_0V_b}{2e}}. \tag{9}$$

Of course, it is impractical to stop an electron beam at the end of a cavity for a number of reasons, including space charge buildup, electron beam velocity spreads, and the danger of reflecting electrons back towards the cathode. Nevertheless, Eqs. (8) and (9) show that the required gap length scales as the square root of the initial electron energy (i.e., directly with the initial electron velocity), and that the electric field scales as $\omega V_b^{1/2}$. Relativistic effects increase the required electric field at higher voltages. In the ultrarelativistic limit, the gap length approaches $\pi c/\omega$, independent of the electron energy, while the gap voltage remains near $\pi V_b/2$. Accordingly, the required electric field scales linearly with electron energy and operating frequency as

$$E_z=\frac{\omega V_b}{2c}. \tag{10}$$

The required electric field in the mildly relativistic regime can be found numerically. The electric field given by Eq. (9) is increased by $\sim$20% at 500 keV and by $\sim$40% at 1 MeV. In recognition of the relativistic modifications to the electron equations of motion, klystron amplifier tubes operating at approximately 500 kV and above are often referred to as relativistic klystron amplifiers (RKAs).

The permitted gap electric field strength is restricted by a breakdown limit, $E_z<E_{br}$, where E_{br}, the breakdown field, depends on the frequency. For low-frequency systems operating in the cw (continuous wave) or long-pulse regime, this dependence was studied by Kilpatrick,[5] who described it by the following equation:

$$f=1.643\times10^{-3}E_{br,cw}^2\exp(-8.5/E_{br,cw}), \tag{11}$$

where the frequency is in GHz and the breakdown field is in MV/m. At high frequencies ($\gtrsim$10 GHz), the exponential term approaches unity, allowing one to rewrite this expression as

$$E_{br,cw}=25f^{1/2}. \tag{12}$$

Experience has shown that it is possible to exceed the Kilpatrick limit by factors of 2 or more.[6] In addition, for short-pulse operation, the breakdown field is further increased. Wilson[7] suggests the following expression:

$$E_{br}(\tau)=E_{br,cw}\left(1+\frac{4.5}{\tau^{1/4}}\right). \tag{13}$$

Here, τ is the pulse duration in μs. Substituting Eq. (12) into Eq. (9) yields the following estimates for the maximum frequency ($f_{\max}$) for long-pulse operation of a single-gap output cavity in the nonrelativistic limit:

$$f_{\max}=\frac{5.6}{V_b}, \tag{14}$$

where f is measured in GHz and V_b in MV. In the ultrarelativistic limit, combining Eq. (12) with Eq. (10) yields

$$f_{\max}=\frac{5.7}{V_b^2}. \tag{15}$$

One common feature of high-power linear-beam devices is multisection output cavities, operating either in a standing- or traveling-wave configuration, in order to lower the required rf fields by progressively extracting the electron kinetic energy in a sequence of gaps. (Note that devices combining input cavities with a traveling-wave output section are also known as twystrons.[8]) In order to localize the EM fields in the resonator, the transverse dimension of the holes in microwave structures (through which the electron beam must propagate without interception) must also be $<\lambda$. This leads to very rapid miniaturization of the interaction volume and the beam cross section with decreasing wavelength. A variety of modifications of the conventional klystron have been suggested to avoid these limitations, including sheet-beam klystrons[9] and multibeam or cluster klystrons.[10]

Another approach to high-power klystrons, using multikiloamp annular electron beams, was developed at the Naval Research Laboratory (NRL).[11] Friedman and co-workers studied the propagation of an intense relativistic electron beam passing through a set of cavities in a cylindrical drift tube. In this situation, the effects of electron-beam space charge are very strong, and changes in wall radius significantly affect the electron energy and the velocity of electron propagation in the tube. They discovered a modulation of the electron beam current, and demonstrated that this ''automodulation'' was due to reflexing electrons caused by virtual-cathode formation in the cavities.[12] When a means was devised to extract microwave power from the modulated beam into an output waveguide,[13] the device became known as a relativistic klystron oscillator (RKO), and later developments led to an amplifier configuration which we will refer to as an intense beam, or high-perveance RKA. We will discuss virtual-cathode formation in Sec. II C in our discussion of vircators, and discuss perveance in our discussion of electron guns in Sec. III B. For that reason, it is convenient to postpone a more complete discussion of the physics of high-perveance RKAs until Sec. IV D 2, where we also present recent experimental results on these high-peak power microwave amplifiers.

Certain devices based on a transversely scanning electron beam also belong to the family of devices based on transition radiation. These devices are generally referred to as ''scanning-beam'' or ''deflection-modulated'' devices. Like klystrons, these devices include an input cavity where electrons are modulated by the input signal, a drift space free from microwaves, and an output cavity in which the electron beam is decelerated by microwave fields. However, unlike

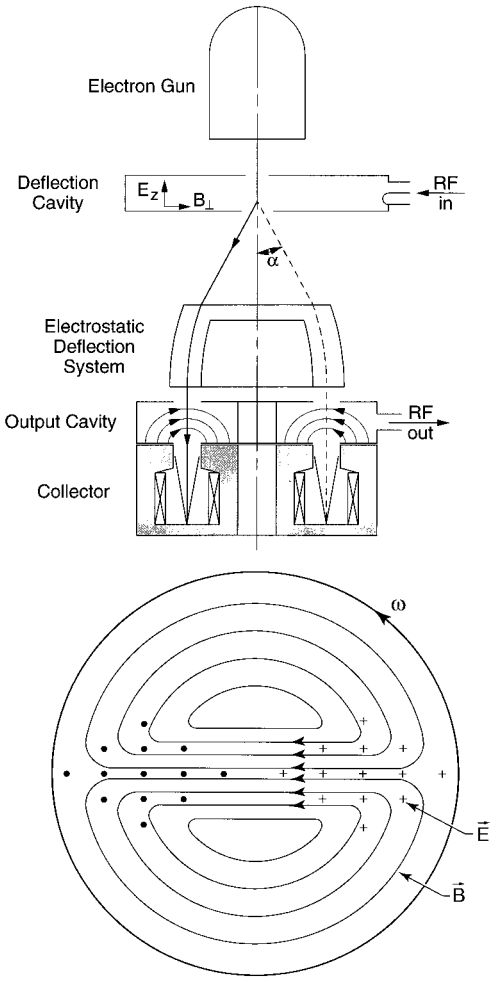

FIG. 4. (a) Schematic diagram of a gyrocon, showing the electron gun, circular deflection cavity, electrostatic deflection system, output cavity, and collector (after Ref. 15); (b) cross sectional view of the deflection cavity, showing the rf fields of a rotating TM_{110} mode.

klystrons, axial bunching is not involved. Instead, an initially linear electron beam is deflected by the transverse fields of a rotating rf mode in a scanning resonator. Since this deflection is caused by the near-axis fields of a circularly polarized rf mode, the direction of the deflection rotates at the rf frequency. After transit through an unmagnetized drift space, the transverse deflection produces a transverse displacement of the electron beam, which then enters the output cavity at an off-axis position that traverses a circle about the axis at the rf frequency. The output cavity contains a mode whose phase velocity about the axis is synchronous with the scanning motion of the electron beam. When the transverse size of the beam in the output cavity is much smaller than the radiation wavelength, all electrons will see approximately the same phase of the rotating mode, creating the potential for a highly efficient interaction. The idea for such a device, the gyrocon, based on the transverse deflection of the beam by the rf magnetic field of a rotating TM_{110} mode (see Fig. 4), was originally suggested by Budker, and several successful experiments were carried out, reaching efficiencies of 80%–90%.[14] These are the highest efficiencies ever achieved in high-power microwave devices. However, the output cavity of this device is subject to the same gap voltage limita-

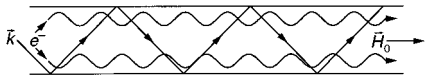

FIG. 5. Schematic diagram of a generic cyclotron resonance maser configuration: a beam of electrons gyrating in a constant magnetic field interacts with an EM wave propagating at a Brillouin angle α_B, where $\cos\alpha_B = k_z c/\omega$.

tions as the klystron, since the electrons interact with the parallel component of the rf electric field. (The rf magnetic field is compensated by dc magnetic field lines, shown in Fig. 4, that are produced by magnetic windings and iron pole pieces enclosing the collector.) In addition, the requirement for a long unmagnetized drift space restricts this device to high-voltage, low-current (i.e., low-perveance) electron beams. A more advanced scanning-beam device known as the magnicon[15] that avoids these limitations is discussed in Sec. IV.

C. Bremsstrahlung

Bremsstrahlung occurs when electrons oscillate in external magnetic and/or electric fields. In bremsstrahlung devices, the electrons radiate EM waves whose Doppler-shifted frequencies coincide either with the frequency of the electron oscillations, Ω, or with a harmonic of Ω:

$$\omega - k_z v_z = s\Omega. \tag{16}$$

Here, s is the resonant harmonic number. Since Eq. (16) can be satisfied for any wave phase velocity, it follows that the radiated waves can be either fast (i.e., $v_{ph} > c$) or slow. This means that the interaction can take place in a smooth metal waveguide and does not require the periodic variation of the waveguide wall that is required to support slow waves. Fast waves have real transverse wave numbers, which means that the waves are not localized near the walls of the microwave structure. Correspondingly, the interaction space can be extended in the transverse direction, which makes the use of fast waves especially advantageous for millimeter-wave and submillimeter-wave generation, since the use of large waveguide or cavity cross sections reduces wall losses and breakdown restrictions, as well as permitting the passage of larger, higher power electron beams. It also relaxes the constraint that the electron beam in a single cavity can only remain in a favorable rf phase for half of a rf period (as in klystrons and other devices employing transition radiation). In contrast with klystrons, the reference phase for the waves in bremsstrahlung devices is the phase of the electron oscillations. Therefore, the departure from the synchronous condition, which is given by the transit angle $\theta = (\omega - k_z v_z - s\Omega)L/v_z$, can now be of order 2π or less, even in cavities or waveguides that are many wavelengths long.

Coherent bremsstrahlung can occur when electron oscillations are induced either in constant or periodic fields. The best known devices in which electrons oscillate in a constant magnetic field are the cyclotron resonance masers (CRMs) illustrated in Fig. 5. This figure shows a hollow electron beam undergoing Larmor motion in a constant axial magnetic field and interacting with an electromagnetic wave whose wave vector is at an arbitrary angle with respect to the

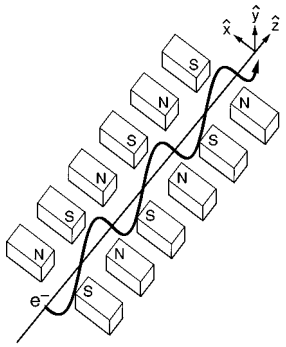

FIG. 6. Schematic diagram of an electron beam passing through a linear wiggler magnetic field. The cross product of the axial velocity along the z axis and the periodic wiggler magnetic field in the x direction produces wiggle motion in the y-z plane.

axial magnetic field. The most common devices based on radiation from electrons oscillating in periodic external fields (see Fig. 6) are free-electron lasers (FELs), also known as ubitrons. For CRMs, in Eq. (16), Ω is the electron cyclotron frequency, $\Omega = eH_0/m_0 c\gamma$, where H_0 is the applied axial magnetic field; and for FELs, $\Omega = k_w v_z$, where $k_w = 2\pi/\lambda_w$ and λ_w is the period of a spatially varying undulator or wiggler magnetic field.

In bremsstrahlung devices, the electron bunching can be due to the effects of the EM field on both the axial velocity of the electrons, v_z, which is present in the Doppler term, and on the oscillation frequency, Ω, since both cause changes in the phase relationship between the oscillating electrons and the wave. In FELs, the oscillating frequency is proportional to v_z. Therefore, changes in the electron energy/velocity can only cause departures from the initial synchronism. In CRMs, the situation is somewhat more complicated because changes in electron energy cause opposite changes in the Doppler term and in the electron cyclotron frequency (which is inversely proportional to the energy). As a result, these changes partially compensate each other, and in the particular case of waves that propagate along the axis of the guiding magnetic field with a phase velocity equal to the speed of light ($k_z = \omega/c$), these two changes cancel each other, as follows from Eq. (16). This effect is known as autoresonance.[16]

One can design a CRM to operate using either fast or slow waves. For slow-wave CRMs, the dominant effect is the axial bunching due to the changes in the Doppler term, while for fast-wave CRMs, the dominant effect is the orbital bunching caused by the relativistic dependence of the electron cyclotron frequency on the electron energy. Cyclotron masers in which this mutual compensation of these two mechanisms of electron bunching is significant ($k_z \sim \omega/c$) are called cyclotron autoresonance masers (CARMs).[17] In these devices, the rate that the electrons depart from synchronism during the process of electron deceleration is controlled by the axial wave number k_z. In both FELs and CRMs, the presence of the Doppler term causes the interaction to be sensitive to the initial axial velocity spread of the electron beam. However, the most common version of the CRM, the gyrotron, operates in the opposite limiting case of very small $k_z (\ll \omega/c)$. The gyrotron is a CRM in which a beam of elec-

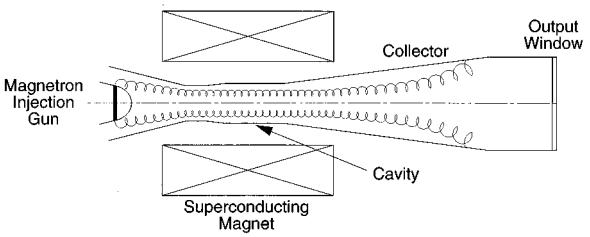

FIG. 7. Schematic diagram of a gyromonotron.

trons moving in a constant magnetic field (along helical trajectories) interacts with electromagnetic waves excited in a slightly irregular waveguide at frequencies close to cutoff. This type of operation mitigates the negative effect of electron axial velocity spread on the inhomogeneous Doppler broadening of the cyclotron resonance band. However, gyrotron oscillators remain sensitive to electron energy spreads. The physics of the interaction between gyrating electrons and fast electromagnetic waves in CRMs was discussed in Refs. 18 and 19. A single-cavity gyrotron oscillator is often referred to as a gyromonotron. This configuration is shown in Fig. 7.

Gyrodevices, like linear-beam devices, have many variants. The most important of them are shown in Table I, which is similar to that shown by Flyagin *et al.* in Ref. 18. From this table, one can see the similarity between known linear-beam devices and their gyrotron counterparts. Note that this table specifically treats gyrotron variants, i.e., CRMs operating in the small-k_z limit, but that it would apply equally to the higher-k_z CARM variants. Furthermore, a similar analogy can be made with FEL variants, so that, more generally, the table is establishing the similarity between linear-beam devices and families of related bremsstrahlung devices.

In FELs, as well as in CRMs operating far from autoresonance, even small changes in the energy of relativistic electrons can lead to disturbance of the resonance condition given by Eq. (16). This restricts the interaction efficiency. The resonance between the decelerating electrons and the EM wave can be maintained by tapering the external fields that determine the oscillation frequency, Ω (i.e., the strength of the guide magnetic field, in the case of a CRM, or the strength or wave number of the wiggler field, in the case of an FEL) and/or by the profiling of the walls of the microwave structure that determine the axial wave number k_z in Eq. (16). This concept is based on the initial formation of an electron bunch in the first section of the interaction region in which the external fields and the structure parameters are constant. Then this section is followed by the second stage in which these parameters are properly tapered for significant resonant deceleration of the bunch trapped by the large amplitude wave. This concept is widely used in FELs[20] and is also studied for CRMs.[21]

Devices based on bremsstrahlung benefit the most from relativistic effects. There are two relativistic effects that can play an important role in them. The first is the relativistic dependence of the electron cyclotron frequency on energy. This effect, which leads to bunching of the electrons in gyrophase, is the fundamental basis of CRM operation. It is interesting to note that in gyrotrons [CRMs in which the Doppler term in Eq. (16) can be neglected], this relativistic effect is the most beneficial at low voltages. To explain this, let us consider the cyclotron resonance condition, assuming that the deviation of the gyrophase with respect to the phase of the wave should not exceed 2π:

$$|\omega - s\Omega| \frac{L}{v_z} \lesssim 2\pi. \tag{17}$$

Since changes in electron cyclotron frequency and energy are related as

$$\frac{\Delta\Omega}{\Omega} = -\frac{\Delta\gamma}{\gamma},$$

the restriction on the deviation in $\Delta\Omega$ leads to the conclusion that all of the kinetic energy of the electrons can be extracted by the EM field without violating Eq. (17) when the operating voltage V_b and the number of electron orbits $N = \Omega L/2\pi v_z$ are related as

$$\frac{eV_b}{m_0c^2\gamma_0} \sim \frac{1}{sN}. \tag{18}$$

This demonstrates that at low voltages, the number of electron orbits required for efficient bunching and deceleration of electrons can be large, which means that the resonant interaction has a narrow bandwidth, and that the rf field may have moderate amplitudes. In contrast with this, at high voltages, electrons should execute only about one orbit. This requires correspondingly strong rf fields, possibly leading to rf breakdown, and greatly broadens the cyclotron resonance band, thus making possible an interaction with many parasitic modes.

TABLE I. Schematics of linear beam devices and corresponding gyrodevices.

Linear Beam Device	Monotron	Klystron	TWT	BWO	Twystron
Type of Gyrotron	Gyromonotron	Gyroklystron	Gyro–TWT	Gyro–BWO	Gyrotwystron

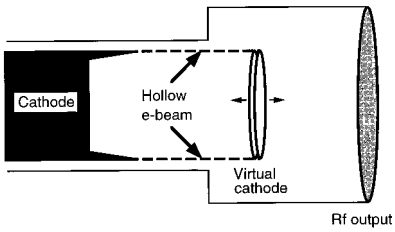

FIG. 8. Schematic diagram of a vircator.

The second relativistic effect is Doppler frequency upconversion. To explain it, let us rewrite Eq. (16) as

$$\omega = \frac{s\Omega}{1 - v_z/v_{ph}}. \tag{19}$$

This shows that when the electron axial velocity is close to the wave phase velocity, the frequency of radiation can be much higher than the resonant harmonic of the electron oscillation frequency. This situation can be realized at low voltages only when electrons interact with slow waves, localized near the structure walls, which leads to the rapid miniaturization of the interaction volume as the wavelength is reduced, as occurs in devices based on Cherenkov and transition radiation. In the case of fast waves, this effect is most pronounced when relativistic electrons interact with waves propagating with phase velocities close to c. In this case, the Doppler frequency upconversion scales with the electron energy as

$$\frac{\omega}{s\Omega} \simeq 2\gamma_0^2.$$

The use of this effect for short-wavelength generation was suggested in the late 1940's by Ginzburg.[22] This frequency upconversion is realized in FELs and CARMs with relativistic electron beams. According to Eq. (19), when the operating voltage is fixed, the operating frequency can be increased either by increasing the resonant harmonic number, s, or by increasing the frequency of electron oscillations. For CRMs, the oscillation frequency is increased by raising the external magnetic field, while for FELs, it is increased by reducing the wiggler period.

Vircators, or virtual-cathode oscillators, constitute a special class of bremsstrahlung device in which the electrons oscillate in electrostatic fields. In the vircator, a high-current electron beam propagates into a region in which space-charge depression limits the current to a lower value. This is often achieved by a sudden increase in the radius of a cylindrical metal drift tube containing a beam propagating at the space-charge limiting current (see Fig. 8). For a thin annular beam of radius r_b in a tube of constant radius R, this current is given by:[23]

$$I_L = \frac{mc^3}{2e} \frac{(\gamma^{2/3} - 1)^{3/2}}{\ln(R/r_b)}. \tag{20}$$

Note that for highly relativistic electrons, Eq. (20) yields the scaling $I_L \sim \gamma_0$, as mentioned previously in the discussion of the BWO. When an increase in wall radius causes I_L to drop below the beam current, the beam slows and some of the current reverses direction, producing a region of high space-charge density and electrostatic potential depression known as a virtual cathode. Two separate processes of radiation generation can occur in this configuration: the virtual-cathode space-charge cloud produces radiation as it oscillates at its plasma frequency, and electrons radiate as they reflex between the real and virtual cathodes. In general, these mechanisms are competitive and do not occur at precisely the same frequency. The simultaneous operation of both mechanisms can reduce the device efficiency. In the reditron,[24] a variant of the vircator, an anode plate with a thin annular slot for passage of the main electron beam stops the reflected electrons, eliminating the second mechanism, in order to increase the efficiency.

Vircators can be treated as an extreme case of the intense-beam RKAs discussed above,[11] in which the voltage depression caused by space-charge effects significantly enhances the electron velocity modulation and bunching. They are also related to reflex triodes, which contain a third electrode (grid) whose potential is more positive than the anode. Therefore, in the space between the grid and the anode, reflected electrons will appear that will oscillate around the positively charged grid. It is interesting to note that a vacuum tube with a positively charged grid, also known as a Barkhausen–Kurz oscillator, was the first microwave source.[25]

Before closing this section, let us note that our classification of device types is not absolute. For instance, in devices based on transition radiation, the rf field localized in short gaps can be Fourier transformed into a superposition of waves with different axial wave numbers. For short gaps, this superposition can include a significant component of slow waves, some of which can be close to the electron velocities. Correspondingly, the radiation of electrons in such gaps, which we have treated as transition radiation, could be viewed as a kind of Cherenkov radiation. Also, in devices based on Smith–Purcell radiation, a linearly moving electron and its image in a periodically rippled metallic wall form a ''flickering dipole.'' From this point of view, one may formulate an alternative treatment of Smith–Purcell radiation as a type of bremsstrahlung.

III. SOME FUNDAMENTALS OF HPM DEVICES

A practical high-power microwave tube must incorporate a variety of technologies, including a high-voltage power supply, a high-power electron gun, a high-power rf circuit, a suitable rf vacuum window, and an electron-beam collector. If it is part of a system, there are also considerations of high-power waveguides, loads, circulators, antennas, etc. The detailed discussion of these technologies is beyond the scope of this article. However, we note that the description of any high-power microwave device begins with the means used to generate the electron beam, in particular the type of electron gun and the power supply used to drive it. We will discuss these two areas in the context of repetitively pulsed, high-average power and single-shot, high-peak

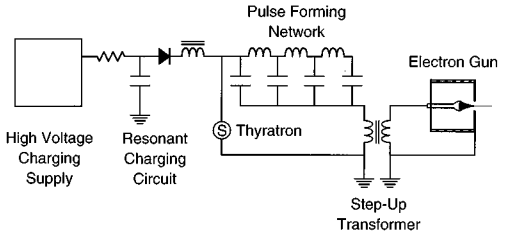

FIG. 9. Schematic diagram of a line modulator.

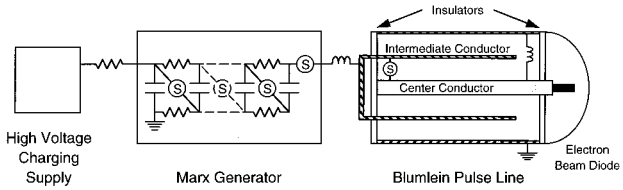

FIG. 10. Schematic diagram of a pulse line accelerator.

power devices, and also give a brief discussion of a critical high-power circuit issue: rf breakdown and other types of pulse shortening.

A. Power conditioning

The power supplies for high-duty factor, repetitively pulsed tubes are generally called modulators. The two basic types are line modulators and hard-tube modulators. The highest power modulators are generally line modulators, and practical devices have been built up to ~ 1 MV output voltage. A typical line modulator configuration is shown in Fig. 9. It consists of a high-voltage power supply, a pulse-forming network (PFN), a switch tube (typically a gas-filled thyratron), and a high-voltage step-up transformer to apply the pulse to the electron gun. Since thyratrons cannot be switched off once they begin to conduct, the pulse shape from a line modulator is controlled by the PFN and the load impedance. Hard-tube modulators use a gridded vacuum tube to switch the high voltage to the electron gun. Since the tube is grid controlled, the pulse shape can be controlled directly, without requiring the use of a PFN. Hard-tube modulators are more flexible, since the pulse shape can be varied without adjusting the PFN. However, gridded tubes can carry much less current than thyratrons (hundreds versus thousands of amps), making hard-tube modulators less suitable for very high-power applications.

The typical single-shot, high-peak power device uses a Marx generator (that is, a set of capacitors that are charged in parallel and discharged in series by means of a set of gas-filled discharge switches), often coupled to a pulse-forming line such as a Blumlein line. (In many Russian systems, such as the SINUS series of accelerators, the Marx generator is replaced by a Tesla transformer, a system of two inductively coupled circuits with equal natural frequencies that can step up the voltage by a factor of more than 1000.[26]) The Blumlein line is used for power multiplication, generally charging from the Marx generator on a microsecond time scale, and discharging into the electron beam diode on a time scale of tens to hundreds of nanoseconds. Such a system is generally referred to as a pulse line accelerator. A typical configuration is shown in Fig. 10. Such systems have been built with voltages greater than 10 MV with high ($>10\ \Omega$) output impedance, and at lower voltages (e.g., a few MV) with fractional ohm output impedances. Another technology that is sometimes used in high-peak power, repetitively pulsed devices is the linear induction accelerator. Its advantage is the ability to progressively accelerate an electron beam in stages, since each module of the accelerator acts like a one-turn transformer, applying a fixed voltage increment to the electron beam, so that there is no limit to the final voltage. (The same technology can be used as a voltage adder to provide higher voltage directly to the cathode, but in this case there is a voltage limit associated with high-voltage breakdown.) One additional pulse-power technology that has been used for high-power microwave generation is the explosive generator, in which the energy stored in high explosives is used to generate a high-voltage pulse by compressing magnetic flux inside a coil. This is one clear limit of the single-shot device, since at the end of the discharge the device has been destroyed. Progress on these devices, which are often called magnetocumulative generators (MCGs), is often reported at the International Conference on Megagauss Magnetic Field Generation (see Ref. 27).

B. Electron gun

The performance of any microwave tube depends critically on the parameters of the electron beam that drives the device. While the potential output power of a device begins with the power of the electron beam, that is, with the product of beam current and voltage, it also depends critically on the achievable device efficiency, which is related to the coherence of the process of decelerating electrons using rf fields. The coherence, in turn, depends on the spatial, energy, and momentum spreads in the electron ensemble that makes up the beam. These spreads are often described generically in terms of the electron beam ''quality.'' Different devices are affected in different ways by these various spreads, and producing a beam with the required current, voltage, spatial dimensions, and beam quality is the first step in building any high power microwave device.

Repetitively pulsed or cw linear-beam devices generally use solid electron beams produced from thermionic electron guns in a Pierce geometry, in which the cathode's emitting surface is a section of the inner surface of a sphere, generally surrounded by focusing electrodes, and electrons are focused in the vicinity of an anode aperture. After current and voltage, the next important measure of the beam produced from a Pierce gun is the final size of the electron beam. Beam size is important because the beam must pass through the transverse dimensions of the rf circuit, which in many devices scale inversely with frequency, as discussed in Sec. II, and also because the spatial variation of rf fields across the beam can affect the performance of the device and lower the interaction efficiency. Minimizing the beam size is critical to the performance of some scanning-beam devices, such as the magnicon, as well as to the extrapolation of other devices, such as thermionic RKAs, to higher frequencies.

Pierce guns can operate either magnetically shielded, or with some magnetic flux linking the cathode. Their performance is limited by the achievable current density of the cathode and by the limit on surface electric fields to avoid high-voltage breakdown. In turn, the current density limit sets the minimum area of the cathode for a particular current, while the achievable beam size depends on the cathode size and on the compression ratio of the electron gun. High-current electron guns with area compression ratios exceeding 1000 have been built,[28] although much lower values of compression are typically employed. However, physics limits the minimum size of an electron beam. For a solid, magnetized electron beam, the minimum beam size is given by the ''Brillouin radius:''

$$r_b = \sqrt{\frac{8Ic^2}{I_A \Omega_0^2 \gamma^2}},$$

where I is the beam current, I_A is the Alfvén current, which is approximately equal to $17000\beta\gamma$ A, c is the speed of light, and $\Omega_0 = eB/\gamma mc$ is the relativistic gyrofrequency in the guide magnetic field. (A nonrelativistic version of this expression is presented in Ref. 29.) This radius corresponds to a rigid-rotor equilibrium with constant axial velocity across the beam, and may be calculated by balancing space charge and magnetic forces for a constant current density beam in the limit of zero transverse emittance and zero canonical angular momentum. (Zero canonical angular momentum corresponds to the case where no magnetic flux links the cathode of the electron gun.)

Transverse emittance is a measure of the transverse phase space occupied by the beam, with coordinates x, y, p_x/mc, and p_y/mc, where $\{x,y\}$ are the transverse dimensions, and $\{p_x, p_y\}$ are the corresponding momenta. The normalized transverse rms emittance in the x direction, which is related to the transverse temperature of the beam, is defined as

$$\epsilon_{xn} = \pi[\langle x^2\rangle\langle (p_x/mc)^2\rangle - \langle x(p_x/mc)\rangle^2]^{1/2},$$

where $\langle ... \rangle$ denotes an average over the electron distribution, and the factor of π is sometimes omitted. A similar expression describes the emittance in the y direction. The rms emittance is often defined including an additional factor of 4 to yield an equivalent ''edge'' emittance. The normalized emittance, which we have denoted here by the subscript n, is conserved if all nonlinear forces, including interparticle forces, may be neglected.[30] An alternative definition of emittance that is particularly useful in interpreting experimental data, is the ''effective emittance,'' which is defined as the area in phase space of the minimum ellipse enclosing $\sim$90% of the beam particles. The beam emittance can increase as the beam experiences nonlinear fields, thus degrading the beam quality. Any real beam has a nonzero emittance due to the effects of a finite cathode radius, cathode roughness, and space-charge fields, as well as to the finite temperature of the emitting surface. Several different definitions of emittance have been discussed in the literature. Useful discussions of emittance, and some of the different ways to define it, are presented in Refs. 31–33. It is also important to note that, while emittance and energy spread are useful global beam parameters that can be used to define the overall beam quality, more specific measures of the beam phase space must be employed to accurately predict the gain or efficiency of particular rf devices.

Gyrotrons and other gyrodevices generally use temperature-limited magnetron injection guns (known as MIGs or MIG guns), in which the electrons are emitted from a cathode strip that is wrapped about the outer surface of a conically shaped cathode (see Fig. 7). The emitted electrons are accelerated by an electric field which, in the vicinity of the cathode, is perpendicular to the cathode surface. Under the action of this field, the electrons acquire an initial velocity whose components parallel and perpendicular to the lines of the magnetic field $\mathbf{B}_0$ depend on the angle between these lines and the emitter surface. Just as in any other gun, the total current achievable from a MIG is limited by the area of the emitting strip, which is determined by its width along the cathode surface and by the mean diameter of the cathode at the location of the strip. (The width of the strip will in turn have some effect on the final beam quality by creating a spread in electron guiding center radii.)

In the transition region between the gun and the microwave circuit, the electrons are accelerated by the electric field up to their final energy. (Many MIGs use an additional electrode, often called the ''modulating anode'' or ''mod'' anode, located radially outward from the cathode, and biased somewhere between the cathode and anode potentials, to control the final ratio of the transverse to parallel momentum, $\alpha = p_\perp/p_z$.) At the same time, the transverse electron momentum in this region changes in accordance with Busch's theorem, which says that in a cylindrically symmetric system, the canonical angular momentum, P_θ, is conserved. P_θ is the sum of the mechanical angular momentum of the particles plus a contribution from the electromagnetic fields, and may be written as

$$P_\theta = \gamma m r^2 \dot{\theta} + erA_\theta,$$

where r is the radius, $\dot{\theta}$ is the angular velocity, and A_θ is the azimuthal component of the vector potential. As a result of Busch's theorem, as the magnetic field is increased to the value necessary to satisfy the CRM resonance condition in the interaction region, the beam α will also increase, while at the same time the mean radius of the annular electron beam may be compressed to a size consistent with the requirements of the rf circuit. Since in gyrotrons, the microwave field mainly extracts the electron kinetic energy associated with the transverse momentum, it is generally desirable to make the beam α as large as possible. Typically, the mean value of α realizable in MIGs is in the range of 1–2, depending on the electron velocity spread. When the spread is large, and the mean value of α is high, some electrons with small initial parallel velocities will be reflected from the magnetic mirror in the transition region; this can cause beam instabilities and thus degrade the beam quality. As discussed previously, gyromonotrons, which operate in the low k_z limit of CRMs, are somewhat insensitive to axial velocity spread, but are sensitive to total energy spread. However, gyroamplifiers, especially those operating at higher k_z, such as CARMs, are particularly sensitive to axial velocity spreads. Some of

the MIG design tradeoffs are discussed in Ref. 34 and references therein. (Note that the basic MIG configuration can also be used to produce a ''Brillouin hollow beam'' with low transverse momentum for use in devices such as TWTs and multicavity klystrons.[29])

The principal cathode type used in high-average power devices is the thermionic cathode. (Secondary-emission cathodes, which are used in cross-field devices such as magnetrons, will not be discussed here.) Emission from cathodes is subject to two basic limits. One relates to the maximum current density that can be drawn from a surface based on its temperature and work function, and is referred to as the temperature limit. (The work function is the energy required to extract an electron through the metal-vacuum interface.) Temperature-limited emission is subject to the Richardson–Dushman equation:[35]

$$J = AT^2 e^{-\phi/W_T},$$

where J is the current density in $\mathrm{A\,cm^{-2}}$, $A = 120\ \mathrm{A\,cm^{-2}\,K^{-2}}$, T is the temperature in degrees Kelvin, ϕ is the work function of the surface in electron volts (eV), and W_T is $T/11\,600$ eV. In general, high current density requires the use of low-work function surfaces, made of materials that can be raised to high temperatures. Typical cathodes operate at temperatures of 1000–1200 °C. The two main types of thermionic cathodes are oxide and dispenser cathodes. The best long-life thermionic cathodes are generally limited to $\sim 10\ \mathrm{A/cm^2}$ current density.

The second limit on current relates to the maximum current that can be drawn across a gap at a particular applied voltage, and is referred to as the space-charge limit. For a planar gap with spacing d and an applied voltage V, this is the Child–Langmuir law, in which the current density scales (in the nonrelativistic limit) as $J = kV^{3/2}/d^2$, where k has a value of $2.33 \times 10^{-6}\ \mathrm{A/V^{3/2}}$. (An exact relativistic solution for the planar diode in terms of elliptic integrals is given by Jory and Trivelpiece.[36]) The perveance of an electron gun, which, in the nonrelativistic limit depends only on the geometry for a space-charge limited gun, is defined as the total beam current (in amps) divided by the 3/2 power of the voltage (in volts). The usual unit for perveance is the μperv, which is defined as $10^{-6}\ \mathrm{A/V^{3/2}}$. (A relativistic generalization to the concept of perveance is given by Lawson.[37]) Recent reviews of thermionic electron gun technology are presented in Refs. 38 and 39.

The goal of achieving very high peak powers in short rf pulses pushes device design in a different direction, since it requires the use of very high-power electron beams. One approach is to use high-voltage, low-impedance drivers, and very low-impedance (high-perveance) electron guns. For this purpose, a variety of ''cold,'' or plasma-covered cathodes have been developed, that rely on explosive electron emission to produce a plasma that is then the source of the electron beam. The current density from explosive-emission cathodes can exceed that from thermionic cathodes by many orders of magnitude. However, in most of these devices, particularly those operating at current densities greater than $100\ \mathrm{A/cm^2}$, plasma expansion (typically several $\mathrm{cm/\mu s}$) leads to closure of the anode-cathode gap, progressively lowering the diode impedance, until the gap is a short circuit. In most cases, this limits explosive-emission cathodes to pulses substantially under 1 μs. Furthermore, the strong electric fields typical of these electron guns generally precludes the use of Pierce or MIG geometries, since it is not possible to suppress emission from the high-field surfaces of focusing electrodes. Other types of cathodes that are under development for high-current density applications in microwave devices are microstructured field emitters[40] and ferroelectric cathodes.[41] (rf guns, including those employing laser photocathodes to produce ultrahigh-brightness electron beams, have found little use in HPM devices, and are thus beyond the scope of this article.)

C. Pulse shortening

It is a common phenomenon in high-power microwave tubes for the duration of the output pulse to be shorter than that of the voltage pulse that is used to drive the electron beam diode. The term ''pulse shortening'' is generally used to describe any case in which the power of the output microwave pulse falls off, or vanishes completely, before the end of the voltage pulse that is used to create the electron beam. (A delay in the start of the microwave signal, due to finite cavity fill times, beam transit times, instability growth rates, etc., is a separate phenomenon.) Pulse shortening can occur for a wide variety of reasons in different microwave devices, and its parameters are very device specific. In some cases, particularly for devices involving explosive-emission cathodes, one of the relevant factors can be the behavior of the electron-beam diode, and the time variation of the electron-beam parameters, while in others, the limiting factors are more directly related to effects that take place in the rf circuit and to the beam-wave interaction.

The emission geometry of explosive-emission diodes is time dependent, because of cathode plasma and possibly anode-plasma expansion, and thus beam properties such as perveance, emittance, and even beam dimensions can evolve during the voltage pulse. (The collapse of the diode impedance can also shorten the voltage pulse, ending the microwave emission.) The deceleration of a high-voltage electron beam to generate microwave radiation involves the use of strong rf fields, often associated with rf cavities or slow-wave structures. These fields can result in rf breakdown (field emission) in the rf circuit, causing the generation of plasmas. (In addition, high fields can cause breakdown in windows, couplers, and other components.) More generally, plasmas can result from the deposition of electron energy in the electron beam collector, or due to scraping of some beam electrons on rf structures or drift spaces. In many cross-field devices, the electron beam is actually collected in the vicinity of the rf structures, increasing the magnitude of this problem. In general, plasmas within the rf circuit can act as time-dependent nonlinear loads on the circuit, and can detune or even completely short out rf structures. For instance, a recent investigation of pulse shortening in relativistic magnetrons has shown that the radial expansion of the cathode plasma changes the microwave boundary conditions, destroying the magnetron resonance condition and ending the microwave pulse.[42] Another effect that can cause pulse shortening in

HPM devices is the buildup of space charge within the rf circuit, due to the combination of rf fields and axial magnetic fields, as low energy electrons are transversely confined magnetically, and are trapped when they can reach neither the anode nor cathode of the device.[43]

In practical high-power thermionic microwave tube designs, rf breakdown is only eliminated by carefully limiting the maximum surface rf fields, and by the use of ultrahigh vacuums ($<10^{-8}$ Torr) combined with rf conditioning (that is, progressively raising the peak power and the rf pulse length until the maximum operating parameters are obtained). These vacuums are achieved by the use of all metal and ceramic construction, using materials such as OFHC (oxygen-free high conductivity) copper and stainless steel, and subjecting the final construction to a high-temperature bakeout in a vacuum furnace, often at temperatures greater than 500 °C to remove adsorbed gases such as hydrogen. In this case, pulse shortening generally occurs only during the initial conditioning phase of tube operation, and vanishes when the tube is ready for full-power operation. However, in high-peak power devices that operate either single shot, or with low repetition rates, and generally in devices that use explosive-emission cathodes, vacuum techniques are less rigorous, and construction often includes elastomer O rings, vacuum grease, and plastic components. Such devices operate in vacuums that are typically no lower than 10^{-6} Torr, and pulse shortening is generally a persistent phenomenon that limits the duration of the high-power microwave pulse to tens or hundreds of nanoseconds, and thus limits the achievable single-pulse energy.

rf breakdown or other pulse-shortening effects typically limit achievable GW-level pulses to lengths of tens to several hundreds of nanoseconds. Determining its causes and possible cures is often a difficult problem, and most of the documentation on this issue is buried in research papers dealing with the characterization of particular experimental devices. A recent review article by Benford and Benford[44] provides a useful survey of the present understanding of these issues. The general problem of pulse shortening in high-power tubes is a principal focus of a Multidisciplinary University Research Initiative (MURI) Program sponsored by the Air Force Office of Scientific Research (AFOSR),[45] and was the subject of a recent International Workshop on HPM Generation and Pulse Shortening which was held in Edinburgh, UK in June 1997.

IV. PRESENT STATUS OF HPM SOURCES

A. Sources for fusion

Microwave energy is widely used for heating and driving steady-state currents in magnetically confined plasmas for controlled fusion experiments. The three basic methods of resonantly heating such plasmas using electromagnetic radiation are based on the resonance between the radiation frequency and one of three resonant frequencies of a magnetized plasma: the ion cyclotron frequency, the lower hybrid frequency, or the electron cyclotron frequency. Correspondingly, the methods are known, respectively, as ion cyclotron heating (ICH), lower hybrid heating (LHH), and electron cyclotron heating (ECH). For the typical magnetic fields required for plasma confinement in present tokamaks and stellarators, the operating frequencies of sources intended for ICH are in the range of tens of MHz up to 100 MHz; the frequencies of LHH sources are on the order of several GHz, and the frequencies of ECH sources range from about 80 to 200 GHz. Since the total microwave power required for plasma heating in large facilities varies from 1 MW, for a number of existing tokamaks and stellarators, to 100 MW for the International Thermonuclear Experimental Reactor (ITER) Project, the required power from a single tube should exceed 0.5 MW (and still higher values are desirable). The microwave pulse duration should correspond to the energy confinement time of the plasmas, which varies from 0.1 s in old systems to about 100 s in planned tokamaks such as ITER.[46] From this, it follows that the microwave energy per pulse should be in the range of 0.1–100 MJ.

Since the low-frequency region of microwaves required for ICH was mastered many years ago, it is simple enough to find rf tubes (usually gridded tubes) suitable for ICH experiments. The needs for LHH experiments initiated some development in the microwave tube industry. For instance, in Japan, JAERI (Japan Atomic Energy Research Institute), in collaboration with the Toshiba Corporation, developed 2-GHz klystrons for LHH experiments on the JT-60 tokamak. The present LHH system for JT-60 consists of 24 tubes, each delivering 1 MW in 10-s pulses.[47] The upgraded version of this tube generates about 1.5 MW in 2-s pulses at a frequency of 2.17 GHz with an efficiency of close to 50%.[47] For LHH experiments on the Italian tokamak FTU, Thomson Tubes Electroniques (TTE) has developed gyrotrons operating at 8 GHz that produce 1 MW in 1-s pulses with 45% efficiency.[48] A photograph of one of these tubes is shown in Fig. 11. Beginning at the bottom, one can see the cathode plate (to which the cathode stalk is mounted), a white ceramic insulator section, the mod anode, and a second ceramic insulator section, to which the remainder of the tube is attached. The tube itself begins with a downtaper, as the beam is compressed by the increasing magnetic field, followed by the cavity, and an uptaper region that ends approximately at the position where two pumping tubes are attached. The remainder of the tube is a large electron-beam collector, through which the microwaves must pass to reach the output window at the upper end of the gyrotron. The tube has an overall length of 340 cm, and operates in the TE_{51} mode at 85 kV with 27 A beam current.

The gap between 8 and 110 GHz was mastered during the 1980's by Varian (U.S.) and GYCOM (Russia): long pulse, 83-GHz tubes were developed by GYCOM (400 kW, 0.1 s) and cw tubes with powers of at least 200 kW at 28, 56, 60, and 70 GHz were developed by Varian. The history of gyrotron development in the 1980's is discussed in Ref. 49.

The main activity in microwave source development for the plasma heating application is focused on gyrotrons intended for electron-cyclotron heating and current drive at frequencies above 100 GHz. During the 1990's, the microwave energy delivered by gyrotrons operating at frequencies above 100 GHz exceeded 1 MJ per pulse. Thermal management in the cavity, collector, and output window is a key

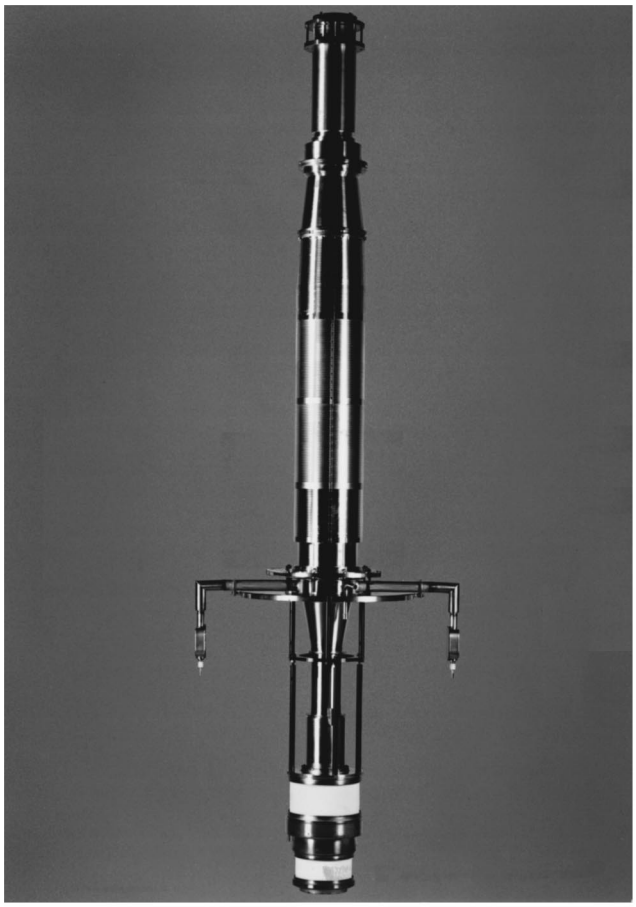

FIG. 11. Photograph of the TTE 8-GHz, 1-MW, 1-s gyrotron shown without its electromagnet and oil tank (photo courtesy of Thomson Tubes Electroniques).

FIG. 12. Photograph of the GYCOM gyrotron ''Centaur,'' with a built-in quasioptical mode converter (after Ref. 52) (photo courtesy of GYCOM).

issue in extending the pulse length of these gyrotrons.

The Russian association GYCOM has developed gyrotrons producing 1 MW at 140 GHz in 1-s pulses and 650 kW in 2-s pulses.[50] These tubes, which operate with an efficiency greater than 40%, are being developed for ECH experiments on the tokamak ASDEX-Upgrade at IPP (Institut für Plasmaphysik, Garching, Germany). Recently, GYCOM developed a 140-GHz gyrotron with a depressed collector. This tube produces 800 kW in 1-s microwave pulses at greater than 50% efficiency.[51] Also, a 110-GHz tube was developed which generates 850, 500, and 350 kW, respectively, in pulse lengths of 2, 5, and 10 s, with approximately 85% of the output power in the TEM_{00} mode. The power limit in each case corresponds to an output window temperature of $<900\,^{\circ}C$.[52] A photograph of this tube, known as ''Centaur,'' is shown in Fig. 12 with its superconducting magnet removed. It is approximately 3 m long, and weighs 250 kg. As in Fig. 11, the electron gun is at the bottom. However, unlike the gyrotron shown in Fig. 11, this tube extracts the microwave power from a window on the side (facing outward in the photo) using a built-in quasioptical mode converter. The region above the window is the electron-beam collector. The U.S. company CPI (Communications and Power Industries, formerly Varian) developed a 110-GHz gyrotron that can generate 680, 530, and 350 kW, respectively, in 0.5, 2, and 10 s pulses.[53] A photograph of this tube is shown in Fig. 13. Again, the electron gun is at the bottom, and the output window is facing outward near the middle of the tube. The remainder of the tube is the electron-beam collector, shaped somewhat differently than for the gyrotron shown in Fig. 12, followed by two vacuum pumps. In Japan, JAERI, in collaboration with Toshiba Corporation, have developed 110-GHz gyrotrons producing 350 kW in 5-s pulses.[54] At 170 GHz, gyrotrons producing 525 and 230 kW, respectively, in 0.6- and 2.2-s pulses were developed by the same team, which also demonstrated the possibility of increasing gyrotron efficiency from 30% to 50% by using a single-stage depressed collector.[55] At 170 GHz, a gyrotron with a depressed collector achieved 38% efficiency at 460 kW.[54] In Europe, a 118-GHz gyrotron for ECH experiments on the tokamaks Tore Supra (France) and TCV (Switzerland) was developed by the Euratom Team, a collaboration between CEA (Commissariat à l'Energie Atomique, Cadarache, France), CRPP (Centre de Recherches en Physique des Plasmas, Lausanne, Switzerland), FZK (Forschung Zentrum Karlsruhe, Karlsruhe, Germany), and TTE (Thomson Tubes Electroniques, Vélizy, France). This tube delivers 450 kW in 5-s pulses and 500 kW in 1-s pulses.[56] It has an output window that is edge cooled with liquid nitrogen. Such cryogenic cooling drastically reduces the microwave losses in the window, making long-pulse, high-power operation possible.

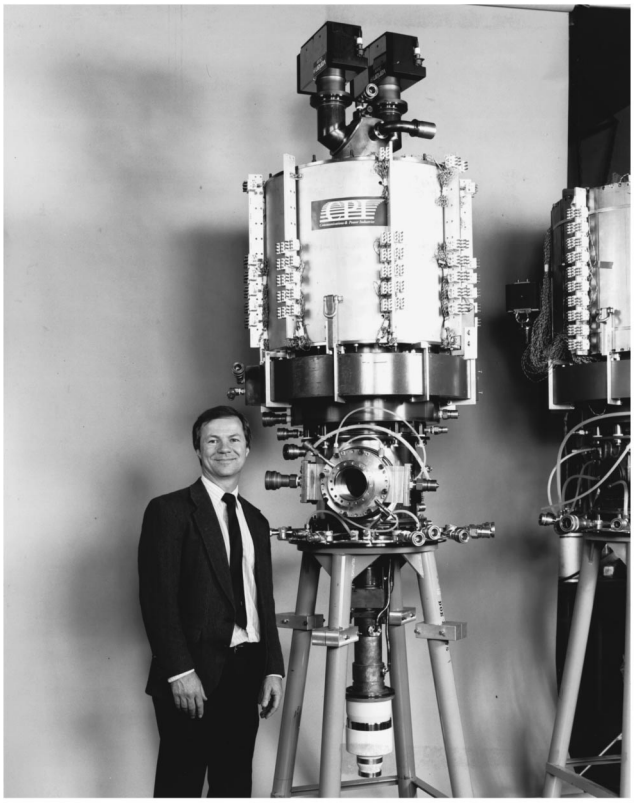

FIG. 13. Photograph of a CPI gyrotron (after Ref. 53) (photo courtesy of CPI).

Table II presents a summary of the recent status of fusion-class gyrotron oscillators.

Another important technical issue for long-pulse (or cw), high-power operation is the separation of the spent electron beam and the microwave radiation in the output section of the tube. This is an issue for gyrotrons, in particular, because the typical gyrotron cavity (except for the quasioptical gyrotron[57]) is a simple cylinder beginning with an uptaper to form the upstream end of the cavity and ending with a second uptaper leading to the output waveguide. Thus, the radiation emerges from the cavity in the same tube as the spent electron beam. Furthermore, even though the transverse dimensions of the gyrotron cavity are already much larger than the wavelength, the collector diameter must be larger, in order to withstand the energy deposition of a multi-MW electron beam. If this transition is done in a tube of variable diameter, as shown in Fig. 7, significant mode conversion of the microwaves will occur. Then, such a mixture of output modes will undergo significant loss in any transmission line. To avoid this problem, almost all long-pulse gyrotrons now use built-in quasioptical mode converters. The idea for such converters, sometimes known as Vlasov couplers, was originally suggested by Petelin and Vlasov at the Institute of Applied Physics (IAP) in Nizhny Novgorod (formerly Gorky), Russia, and is illustrated by Fig. 14, which is taken from Ref. 58. Improved versions of such converters, known as dimpled or Denisov converters,[59] are capable of transforming the high-order modes of gyrotron resonators, such as the $TE_{22,6}$ mode, into linearly polarized Gaussian beams with 95% efficiency. (In the Denisov converter, the dimples modify the electromagnetic wave into a Gaussian profile prior to the reflectors of the quasioptical converter, thus improving the conversion efficiency.) Such beams can propagate with very small losses in oversized waveguides and mirror transmission lines. The Russian tube ''Centaur'' shown in Fig. 12, as well as the CPI tube shown in Fig. 13, include built-in quasioptical mode converters. In the middle of both tubes, one can see an output window through which the microwave power is extracted perpendicular to the tube axis.

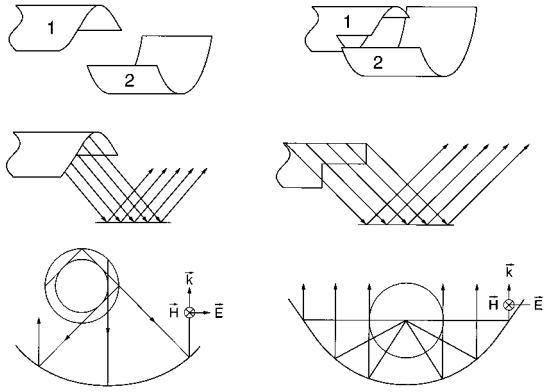

FIG. 14. Schematic diagram of the principal types of quasioptical mode converters: (1) quasioptical antenna, and (2) parabolic reflector. (a) Converter for a whispering-gallery TE_{mn} mode ($m \gg n$); (b) converter for a TE_{0n} or TE_{1n} mode.

B. Sources for linear accelerators

One important application of rf sources is to power particle accelerators. The accelerator application requires high rf

TABLE II. Gyrotrons for electron cyclotron heating and current drive in fusion plasmas at $f > 100$ GHz.

Institution/Country	f (GHz)	P (MW)	τ (s)	η (%)	Ref. No.
CPI (Varian)/U.S.[a]	110	0.68/0.53/0.35	0.5/2/10	31/30/27	53
JAERI+Toshiba/Japan	110	0.35	5	30	54
GYCOM/Russia[a]	110	0.70/0.32/0.29	2/5/10	37/30/	52
Euratom Team/Europe[a]	118	0.5/0.45	1/5	28/25	56
GYCOM/Russia	140	1/0.65	1/2	>40	50
GYCOM/Russia	140	0.8	1	50[b]	51
GYCOM/Russia	160	0.5	0.7	30	50
JAERI+Toshiba/Japan[a]	170	0.52/0.23	0.6/2.2	32[b]	54

[a]Power and efficiency are quoted into the TEM_{00} output mode.
[b]Tube used depressed collector to increase efficiency.

phase stability (typically $<1°$) between all the accelerating cavities. When the total rf power requirement exceeds the capabilities of a single microwave source, this generally requires the use of rf amplifier tubes operating in phase synchronism (although phase-locked oscillators might in principle also meet this need). rf accelerators for protons or heavier ions require low frequencies ($f<1$ GHz), while electron and positron accelerators generally operate at higher frequencies. The Stanford Linear Accelerator Center (SLAC) two-mile electron-positron linear collider (SLC) is driven by approximately 240 SLAC 5045 klystrons at a frequency of 2.856 GHz. These klystrons produce 65 MW in a 3.5-μs pulse at a repetition rate of 180 Hz with an efficiency of 45%, using a 350 keV, 415-A electron beam.[60]

Much of the accelerator-related advanced rf source research has been motivated by the requirements for proposed new accelerators that would collide electrons with positrons at a center-of-mass energy, initially, of 0.5 TeV.[61] This would be upgradable to 1 TeV, and future concepts extend this to 5 TeV and higher. The optimum collider frequency is still under debate, and device concepts involving frequencies between ~ 1 and 90 GHz are under investigation. In general, increasing the rf frequency increases the achievable accelerating gradient, since breakdown field strengths increase with frequency, and the threshold electric field for capture and acceleration of ''dark current'' from the cavity surfaces, a deleterious effect in high-gradient accelerators, also increases with frequency. Wilson gives designs for a 5-TeV center-of-mass collider operating at 34.3 GHz and 10- and 15-TeV colliders operating at 91.4 GHz.[62]

There are at least five major organizations carrying out research on linear collider concepts: SLAC, DESY (Deutsches Elektronen-Synchrotron, Hamburg, Germany), KEK (National Laboratory for High Energy Physics, Tsukuba, Japan), BINP (Budker Institute of Nuclear Physics, Russia), and CERN (European Laboratory for Particle Physics, Switzerland). The research spans eight design concepts, ranging in frequency from TESLA (DESY), a proposed superconducting linac operating at 1.3 GHz to CLIC (CERN), a proposed 30-GHz two-beam accelerator concept in which a set of extraction cavities driven by one electron beam is used to generate the rf for the high-gradient acceleration of a second electron beam. The design under consideration at SLAC, known as the Next Linear Collider (NLC), operates at 11.424 GHz, four times the frequency of the existing Stanford Linear Collider. This frequency is also one of those under consideration at KEK. Table III gives some approximate parameters for a 0.5 TeV NLC, which would make use of 50 MW klystrons and rf pulse compression.

TABLE III. rf parameters for 500 GeV center-of-mass Next Linear Collider (from Ref. 61).

Frequency	11.4 GHz
Unloaded/loaded linac accelerating gradient	50/37 MV/m
Active two-linac length	14.2 km
Klystron peak power	50 MW
Klystron pulse length	1.2 μs
Total number of klystrons	3936
rf pulse compression ratio	5
rf pulse compression gain	3.83
Total rf power after compression	750 GW
rf pulse length after compression	240 ns
Repetition rate	180 Hz
Klystron electronic efficiency	60%
Net efficiency for production of rf power	30%
Total wall-plug power required to make rf	103 MW

There is a considerable research effort under way to develop sources for future linear colliders. The main research effort has been in extrapolating klystron technology to higher powers and higher frequencies. The approximate scaling law for klystron peak power is f^{-2} (based on structure sizes). As a result, the extrapolation of the 2.856-GHz SLAC 5045 klystron to 11.424 GHz, the proposed NLC frequency, amounts to more than an order of magnitude increase in the normalized power. There are also a number of programs aimed at developing alternatives to klystrons that might operate at higher power, higher efficiency, or higher frequencies. The sources for particle accelerators, klystrons, as well as some of the alternatives, such as gyroklystrons and magnicons, will be considered below. Their status is summarized in Table IV. In addition, we will discuss the important subject of rf pulse compression, which permits accelerator designers to increase the peak powers available from microwave tubes.

1. Relativistic klystrons

The term relativistic klystron amplifier (RKA) has been used to describe two very different regimes of klystron op-

TABLE IV. Experimental microwave amplifier tubes for future linear colliders.

Device	f (GHz)	P (MW)	η (%)	τ (μs)	V (kV)	I (A)	Ref. No.
SLAC S-Band Klystrons	3	150	>40	3	535	700	63
TTE Klystron TH 2153	3	150	43	1.2	576	600	64
SLAC XL4 Klystron	11.4	75	48	1.1	450	350	66
SLAC X5011 PPM Klystron	11.4	55	55	1.5	470	213	66
KEK/Toshiba XB72k Klystron	11.4	95/30	33	0.07/0.3	620	~ 550	68
Haimson Research Klystron	17.1	26	49	0.15	560	95	67
BINP Klystron (gridded gun)	14	60	30	0.5	1000	~ 200	69
BINP Klystron (induction linac)	14	100	40	0.25	1000	250	70
UMD Gyroklystron (two cavity)	9.87	24	30	1	425	190	78
UMD Gyroklystron (three cavity)	9.87	27/16	32/37	1	425	100	78
UMD Gyroklystron (two cavity, 2 Ω_c)	19.76	32	29	1	457	244	79
BINP Magnicon	7	46	49	1	405	230	86

eration (see Sec. II). In the devices described here, ''relativistic'' refers principally to the use of high-energy electrons, where relativistic effects modify the usual formulas for klystron bunching. Extracting the electron kinetic energy in a single rf gap becomes increasingly difficult both as the electron energy increases and as the frequency increases, and multisection cavity structures are required. The more complicated mode structure of these cavities often creates instability problems.

The S-Band Linear Collider (SBLC) Program at DESY is investigating the option of building a future collider near the frequency of the present SLC. For this program, SLAC has extended the technology of the SLAC 5045 klystrons to higher current and rf power density in order to develop two 3-GHz, 150-MW, 3-μs klystrons. These klystrons use an $\sim$535 keV, 700 A electron beam, have 55 dB saturated gain, and operate at 60 Hz repetition rate with $>$40% efficiency.[63] Also, Thomson Tubes Electroniques (TTE) has reported an experimental 150-MW, 1.2-μs klystron at 3 GHz, designated TH 2153, with an efficiency of 43% and a gain of 48 dB at saturation.[64]

The main U.S. development program for high-power 11.424-GHz klystrons has been at SLAC. This program began with the XC series of klystrons, that were designed to operate at 100 MW in 1-μs pulses.[60,65] The XC series of klystrons proceeded through eight variants, without ever simultaneously meeting the design power and pulse length. The best results were 87 MW in a 300-ns pulse and 50 MW in a 1-μs pulse.

The program was then redirected to the XL series of klystrons in 1993, where the target was a lower perveance tube (1.2 μperv compared to 1.8 μperv for the XC series) that would operate successfully at 50 MW for a full 1.5 μs. (The section below on Pulse Compression discusses the conversion of this pulse into the 200 MW, $\sim$250-ns pulse required by the NLC.) The XL-4 klystron produced 75 MW with 55 dB gain and 48% efficiency in a 1.1-μs pulse at 120-Hz repetition rate, using a 450-keV, 350-A beam. It required a focusing magnetic field of 0.47 T. The focusing field did not use a superconducting magnet, and required 15 kW of electric power. In order to eliminate this power dissipation, SLAC recently tested a PPM (periodic permanent magnet) focused klystron, designated X5011. This tube, using a 470-keV, 213-A electron beam, has achieved 55 MW with 55 dB gain at 55% efficiency in a 1.5-μs pulse.[66]

A high-power klystron has been developed by Haimson Research Corporation at 17 GHz for use in an experimental laser-photocathode rf gun under development at the Massachusetts Institute of Technology (MIT). This tube produced $>$26 MW of output power in a 150-ns pulse at 49% efficiency, using a 95-A, 560-keV beam, at a saturated gain of 67 dB.[67]

KEK, in collaboration with the Toshiba Corporation, also has a program under way to develop klystrons at 11.4 GHz. Their tube is designated XB72k, and operates at 620 kV, $\sim$550 A. They have operated several prototypes of this tube using both single-gap and traveling-wave output circuits, and have achieved 95 MW in a 70-ns pulse and 30 MW in a 0.3-μs pulse.[68] These short pulse lengths were due to breakdown in the output cavity.

The Protvino branch of the Budker Institute of Nuclear Physics (BINP) has carried out several relativistic klystron experiments at 14 GHz using electron beams of $\sim$1 MeV and $\sim$300 A. In one of these experiments, a power of 60 MW was observed with a pulse length of $\sim$0.5 μs, using an $\sim$1-MeV, 200-A beam from a gridded electron gun using a dc-biased cathode. Its power was limited by self-excitation. This gridded-gun configuration could avoid the loss of overall system efficiency associated with the use of a conventional modulator.[69] In other experiments, an induction accelerator was used to create the electron beam. Those experiments produced $>$100 MW in a 250-ns pulse with 40% efficiency and $\sim$80 dB gain from a 1-MeV, 250-A beam.[70] This klystron had 11 bunching cavities and used a 22-cell output structure with an overall length of 11 cm.

A recent review of high-power klystron design and engineering is presented in Ref. 71.

The Lawrence Berkeley Laboratory/Lawrence Livermore National Laboratory (LBL/LLNL) two-beam accelerator (TBA) concept makes use of a very special kind of RKA. In the TBA, a low-current beam is accelerated to very high energies using microwaves generated by a second higher current electron beam that is operating at more modest voltages. The microwave power is generated by a klystron-type interaction (although the use of an FEL interaction to generate the microwaves in a TBA was first discussed by Sessler[72]). The key to this TBA concept is to use a much higher beam energy (4–10 MeV) than is conventional in other klystrons, and to extract only a small fraction ($<$10%) of the kinetic energy in a single stage, which then drives a fixed length of the high-energy accelerator. The electrons are then reaccelerated in an induction module before being sent through another extraction cavity to generate additional microwave power. If this process can be continued over and over again without severe deterioration of the beam phase space, then the overall efficiency can be quite high, since the spent electrons are continually being reused rather than collected. In the experimental tests of this concept, the beam bunching was produced by transverse deflection of the electron beam across an aperture by the transverse magnetic field of a TM_{110} mode at half of the output frequency, a configuration that was referred to as a ''chopper-driven traveling-wave rf generator'' or ''Choppertron.''[73,74] A series of 11.4-GHz microwave generation experiments was carried out on the ATA induction linac at LLNL at voltages of 2.5–5 MeV and currents of up to 1 kA using a variety of traveling-wave extraction structures. These experiments produced a combined peak microwave power of 180 MW in $\sim$25-ns pulses from a pair of traveling-wave output structures, and 260 MW in shorter pulses. Following this, a reacceleration experiment was carried out (see Fig. 15), in which three output cavities, separated by induction cells pulsed at 250 kV to reaccelerate the beam, produced a total power of $\sim$170 MW in 25-ns pulses, and $\sim$20% higher power in shorter pulses. In a later experiment on ATA, the ''Choppertron II'' produced $>$500 MW at 11.4 GHz in a $\sim$20-ns pulse from a single output structure, using a 4.6-MeV, $\sim$800-A electron beam.[75]

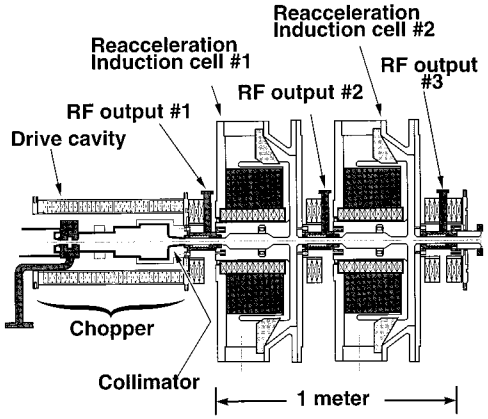

FIG. 15. Schematic diagram of the relativistic klystron two-beam accelerator reacceleration experiment (after Ref. 74), (Source LLNL). A 5-MeV, 1-kA beam enters from the left.

Another TBA concept is under investigation at CERN to generate 30-GHz microwaves for CLIC. In this device, a prebunched electron beam with a total charge of 2.58 μC, generated either from a photoinjector or by using a FEL prebuncher, would be accelerated to 3 GeV, and then progressively decelerated to 350 MeV in a sequence of gaps to generate the required microwave power. A total of $\sim 5 \times 10^{11}$ W would be extracted from each beam at a rate of two 44.6-MW, 11.6-ns pulses from each 50-cm section, with a total efficiency of 72%. The CLIC decelerating structures have been tested using a prebunched 65-MeV beam consisting of 48 electron bunches, each containing 3 nC of charge, and produced 76 MW in a 12-ns FWHM pulse.[76]

2. Gyroklystrons

The gyroklystron is a member of the class of fast-wave gyrodevices discussed in Sec. II. The transverse and axial cavity dimensions can be much larger than a wavelength, allowing these devices to scale to high frequencies better than conventional klystrons. This makes gyroklystrons an attractive candidate for driving future colliders at frequencies above the *X* band (which is conventionally defined as 8–12.5 GHz).

One limitation to these devices is the necessity to create magnetic fields corresponding to the cyclotron resonance condition. When the Doppler term in this condition is small [see Eq. (16)], the required magnetic field can be estimated by a simple formula

$$B_0 \mathrm{T} \approx \frac{1.07 \gamma_0}{s \lambda (\mathrm{cm})}.$$

From this formula, it follows that operation at frequencies above the *X* band requires either the use of superconducting magnets, when operating at the fundamental cyclotron resonance ($s=1$), or operation at cyclotron harmonics ($s>1$), which reduces the magnetic field by s^{-1}. In the latter case, water cooled or permanent magnets might be used. Let us note that the magnetic fields in gyrotrons are comparable to those in high-power klystrons at the same frequency that use magnetically confined flow; however, there is no alternative to the use of strong magnetic fields in gyrodevices, unlike klystrons, in which periodic permanent magnet (PPM) focusing is an alternative.

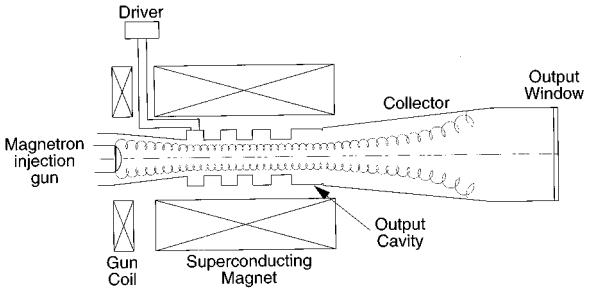

FIG. 16. Schematic diagram of a relativistic gyroklystron.

The development of gyroklystrons for future linear colliders is under way at the University of Maryland (UMD), (See Ref. 77 for a recent review.) In the first set of experiments, *X*-band gyroklystrons (GKLs) operating at the fundamental cyclotron resonance were developed. A typical configuration is shown schematically in Fig. 16. These tubes operated at voltages up to 450 kV and currents up to 200 A with pulse lengths greater than 1 μs. In a series of two-cavity GKLs, the best results were an efficiency of 34%, a power of 24 MW, and a gain of 34 dB. (Operation at 24 MW corresponded to 30% efficiency and 33 dB gain.) In experiments with three-cavity GKLs,[78] the maximum saturated gain was increased to 50 dB at a power of 21 MW, while the maximum power of 27 MW was obtained at 32% efficiency and 36 dB gain, and the maximum efficiency of 37% was obtained at 16 MW and 33 dB gain.

In the next set of experiments, two-cavity second-harmonic gyroklystrons were designed and tested.[79] The output cavities of these tubes operated at ~ 20 GHz, while the input cavities were driven at half this frequency at the fundamental cyclotron resonance. The best performance with a 457-keV, 244-A electron beam corresponded to 32 MW at 29% efficiency with a gain of 27 dB. Note that for this tube, the ratio of the microwave energy per pulse divided by the square of the wavelength, which is inversely proportional to the number of amplifiers required to drive a linear collider (see Ref. 77), was the same as for the best SLAC klystron operating at 11.4 GHz.[65]

A number of experiments were also carried out with relativistic gyrotwystrons. These devices used the same prebunching section as the GKLs (the input cavity and drift region), but the output cavity was replaced by an output waveguide. The gyrotwystron configuration can mitigate the problem of microwave breakdown at high power levels, since the microwave energy density in the output waveguide can be much smaller than in a high-Q output cavity. The physics of relativistic gyrotwystrons was analyzed in Ref. 80. Experiments were carried out in both first and second harmonics. In the fundamental harmonic *X*-band gyrotwystron, a peak power of 22 MW was achieved in a 2-μs pulse with a gain of >25 dB and 21% efficiency.[81] In the second harmonic tube (with prebunching at the fundamental harmonic), 12 MW was produced at 19.76 GHz with 21 dB gain at 11% efficiency. The second harmonic tube was more

susceptible to the excitation of spurious modes.

One of the important features of all these experiments was the proper profiling of the external magnetic field. In GKLs, this profiling should first provide proper conditions for electron prebunching in the input cavity. Next, the magnetic field should be slightly increased in the drift region to reduce the effect of electron axial velocity spread on the orbital bunching of the electrons. Finally, the field should be downtapered in the output cavity in order to compensate for the loss of electron energy to the rf field. In gyrotwystrons, the magnetic field in the output waveguide must be tapered to provide synchronism between an electromagnetic wave and a decelerating electron bunch. (This issue was analyzed in Ref. 82.)

At present, the GKL program is aimed at producing 100 MW at ~8.5 GHz (three times the frequency of the SLC) in a first harmonic tube and ~17 GHz in a second harmonic tube. In order to do this, the modulator was upgraded to 800 A at 500 kV with a 1.5-μs flat top. In order to limit the cathode loading, the emitter strip radius was increased to ~7.5 cm, increasing the beam radius in the interaction space by approximately a factor of 3. In order to maintain intercavity isolation with this large beam radius, a coaxial cavity configuration was used. A number of designs for two- and three-cavity coaxial GKLs are presented in Refs. 77 and 83. These designs predict operation at 100–150 MW with ~40% efficiency in both the fundamental and second cyclotron harmonics. This efficiency can be further improved by using a depressed collector technique.[84] The gain in the three-cavity designs is ~50 dB. These experiments are scheduled to begin in the near future.

3. Magnicons

The magnicon[15,85] is a member of the class of scanning-beam amplifier tubes that includes the gyrocon discussed in Sec. II. However, the magnicon is a magnetized device using a fast-wave output cavity. Therefore, it can also be grouped with gyrotrons as devices in which electrons gyrating in an external magnetic field emit bremsstrahlung radiation near the cyclotron resonance. In the earliest version of the magnicon, an electron beam is deflected using a rotating TM_{110} mode, as in the gyrocon, but after an unmagnetized drift space, the deflected beam is spun up to high transverse momentum by entry into a strong magnetic field at the entrance to the output cavity (see Fig. 17). As a result of the phase-synchronous transverse deflection of the electron beam as a whole, the beam electrons entering the output cavity execute Larmor motion whose entry point and guiding center rotate in space about the cavity axis at the drive frequency. In the output cavity, the beam is used to drive a cyclotron-resonant fast-wave interaction with a synchronously rotating TM_{110} mode that extracts principally the transverse beam momentum. This interaction can be highly efficient, because the magnicon beam is fully bunched in space and in gyrophase, so that the phase bunching produced by the cyclotron maser instability is not required. With all of the electrons decelerated identically, very high efficiencies can be achieved. The first magnicon was developed by Nezhevenko and coworkers at the BINP, and produced 2.6 MW at 915 MHz

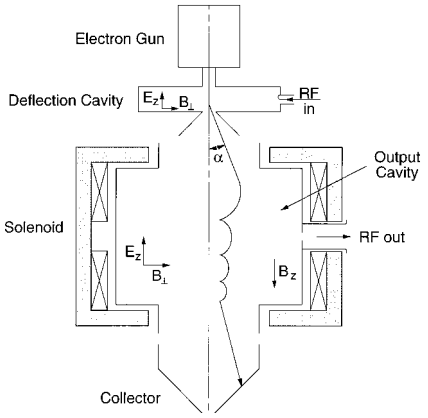

FIG. 17. Schematic diagram of a magnicon (after Ref. 15), showing the electron gun, deflection cavity, solenoid, output cavity, collector, and the complete trajectory of an electron deflected at an angle α in the deflection cavity.

with 73% efficiency, using a 300-keV, 12-A electron beam (7×10^{-2} μperv).[85] A 1.3-GHz variant of this basic design is of interest to power the proposed superconducting TESLA linac at DESY.

Recently, new higher perveance versions of the magnicon have been developed, in which a fully magnetized electron beam is spun up to high transverse momentum in a sequence of deflection cavities containing synchronously rotating TM_{110} modes, the first driven by an external rf source. In addition, the output cavity can operate in the mth harmonic of the drive frequency by using TM_{m10} modes with $m>1$, permitting extension of magnicon operation to higher operating frequencies. The key to the efficiency of these new magnicon designs is to spin the beam up to high transverse momentum ($\alpha>1$) without producing large spreads in energy and gyrophase, so that the output cavity interaction will remain coherent over the entire ensemble of electrons, and not just synchronous in time. This requires great care in the design of the deflection cavities, in particular of the penultimate deflection cavity that produces more than half of the beam spin up. Since these spreads are generated by the fringing fields of the beam tunnel apertures in the deflection cavities and the output cavity, it also requires the use of a very small initial beam radius.

There are two groups developing magnicons for the accelerator application, one at the BINP in Novosibirsk, Russia, and the second at NRL. The BINP magnicon program is developing a frequency-doubling magnicon configuration with an output frequency of 7 GHz, and has reported 46 MW at 49% efficiency in a 1-μs pulse at a repetition rate of 3 Hz, using a 405-keV, 230-A electron beam.[86] Their device is based on a conventional modulator and ultrahigh-convergence thermionic electron gun.

NRL is developing a similar frequency-doubling configuration with an output frequency of 11.4 GHz. In a preliminary experiment, NRL reported 14 MW at 10% efficiency at 11.16 GHz, using a 650-keV, 225-A beam from a cold-cathode diode driven by a single-shot Marx generator.[87] However, plasma loading of the deflection cavities limited operation to a regime in which the penultimate cavity was

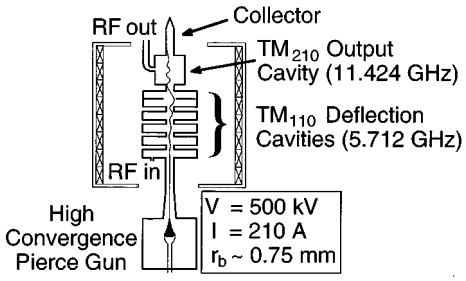

FIG. 18. Schematic diagram of a frequency-doubling magnicon amplifier configuration.

unstable. A new 11.424-GHz magnicon experiment is being built at NRL (see Fig. 18), using a modulator and a novel ultrahigh-convergence thermionic electron gun to produce a 500-keV, 210-A, 1.5-mm-diameter electron beam with a 1.5-μs pulse length at a 10-Hz repetition rate.[88] Simulations suggest that powers approaching 65 MW at $>60\%$ efficiency should be achievable.

Recent work has suggested that magnicon operation may be scaled to still higher frequency (e.g., 34 GHz) by operating the output cavity in the third or fourth harmonic of the drive frequency.[89,90]

4. Pulse compression

The concept of compressing rf pulses in time in order to increase their peak power is not new. The common motivation for this is that it is ''easier'' to generate lower peak powers at longer pulse lengths, since this can be done using lower current and voltage electron beams, and requires lower circuit rf fields. One means to compress a rf pulse is to store the microwave energy in a cavity, and rapidly switch it out by changing the cavity Q. References to this work go back to the early 1960's (see Ref. 91 and references therein). Alvarez *et al.* produced 150 kW, 2-μs pulses at 8.2 GHz by storing energy from a 300 W drive source in a 7-cm radius superconducting cavity, and then using a mechanical plunger to change the cavity Q.[92] However, simple cavity schemes can lead to very high rf fields and to rf breakdown, if used with high-power pulses. A variety of approaches have been studied to compress high-power pulses while avoiding rf breakdown. One of these is binary pulse compression, in which phase encoding is combined with 3-dB hybrid couplers and variable delay lines to produce one or more stages of power doubling.[93] Another is the SLED (SLAC Energy Development) and SLED II configurations developed at SLAC, in which a pair of storage cavities connected by a 3 dB coupler are rapidly emptied by a 180° phase shift of the drive signal.[94] In the SLED II pulse compressor (see Fig. 19), the cavities are long lengths of oversized circular waveguide (WC-475), operating in the low-loss TE_{01} mode and shorted at the ends. The SLED II pulse compressor that is now used

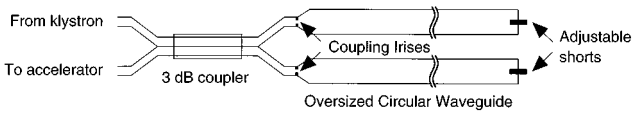

FIG. 19. Schematic diagram of a SLED II pulse compressor.

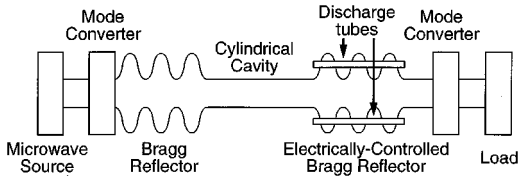

FIG. 20. Schematic diagram of a microwave pulse compressor with Bragg reflectors (after Ref. 96).

at SLAC on the Next Linear Collider Test Accelerator (NLCTA) employs ~36-m-long cavities to compress a 50-MW, 1.5-μs pulse by a factor of ~5 with 80% efficiency, yielding a power increase of ~4.

Similar parameters were also realized in an open cavity pulse compressor system that was developed at the Protvino branch of the BINP, first for the VLEPP accelerator (Russia) and then for the Japan Linear Collider (JLC) located at KEK.[95] In this system, the key element is an open cylindrical cavity that is excited through coupling slots by a waveguide wrapped around the cavity perimeter. The slots excite a whispering-gallery mode propagating in the cavity as a traveling wave localized near the cavity wall. Phase velocities in the waveguide and cavity are matched by adjusting the width of the waveguide. Cavity Q factors as high as 10^5 can be realized in this highly selective open cavity configuration by increasing the cavity diameter while limiting the density of the mode spectrum. In such systems, 31-MW, 500-ns microwave pulses from an 11.4-GHz JLC klystron were compressed into 134-MW, 110-ns pulses with 69% efficiency.

Another approach to high-power, high-frequency pulse compression is based on the use of oversized open cavities with a variable reflection coefficient at one end.[96] In contrast to conventional switched-energy storage pulse compressors, the new systems do not contain any small-size elements. This allows them to operate without breakdown at high power levels. An example of such a system is shown schematically in Fig. 20. Here a cylindrical cavity, in which the microwave energy is stored, is placed between two Bragg reflectors providing very low transmission coefficients. A set of gas discharge tubes is placed along the Bragg reflector on the right-hand side of the cavity, to form an output switch. These tubes can be switched on in 5–10 ns, making the Bragg reflector transparent to microwaves, and causing the cavity to empty. The total length of such an *X*-band compressor can be only several meters. Theoretical analysis[96] shows that such a system can operate with an efficiency of 70%–80%, producing >100-MW, 100-ns pulses with a compression ratio of ~10.

C. Sources for radar and communications systems

Radar systems locate and characterize distant objects by radiating electromagnetic energy from an antenna in the direction of the objects and detecting and measuring the reflected signals. While many of the advances in radar systems over the past 50 years relate to the improved processing of the returned signal, some of the more recent advances in radars are based on the development of two classes of HPM sources: high-peak power, short-pulse (ns) sources and longer pulse (μs) millimeter-wave sources. We present an

introduction to the use of these sources in connection with modern radar systems. The interested reader is referred to Ref. 97 for a more detailed discussion.

1. Short-pulse radars

The principal advantage of short-pulse radars is in range resolution.[98] Conventional radars achieve range resolution using long microwave pulses by radiating a pulse with a frequency chirp, Δf, (or other encoding) and using digital pulse compression of the received signal to provide an effective pulsewidth of approximately $1/\Delta f$.[99] However, the signal processing of the received signal introduces temporal side lobes that can mix signals from nearby range cells. As a result, the received signal from a large cross-section object can conceal signals from smaller targets in its proximity. This problem does not occur with short-pulse radars, because the received signal does not require pulse compression. Since radiation propagates 30 cm in 1 ns, it is evident that the operation of radars with a few nanoseconds pulse duration can provide 1-m range resolution directly. This can help to detect low-reflection moving objects in the presence of substantial radar ''clutter.''

Another advantage to nanosecond radars follows from the fact that the radar receiver must be turned off during the pulse duration of the high-power transmitter, in order to protect the receiver electronics. In short-pulse radars, this ''dead time'' is small. Note that in some cases, to provide the required average power, short-pulse radars must operate at high repetition rates.

The development of repetitively pulsed, nanosecond HPM sources began in the former Soviet Union (FSU) in the 1970's.[100] First, an *X*-band relativistic BWO was developed by the IAP and the Institute of High Current Electronics (Tomsk). This tube produced 0.5 GW of microwave power in single 5-ns pulses from a 500-keV, 10-kA electron beam, and 100-MW pulses at a 100-Hz repetition rate. The pulse-to-pulse stability required for subtracting subsequent pulses from one another (in order to separate moving targets from clutter) was provided by stabilizing the beam voltage and current to 1%. The operation of an *X*-band radar based on such a BWO was first demonstrated on the bank of the river Ob near Tomsk, Russia.[98,101] That radar could detect a small airplane (effective cross section $\sim 1\ \mathrm{m}^2$) in a direct line of sight at a distance of 50 km, and small boats could clearly be seen among the waves and islands of the river. An improved version of this radar, called NAGIRA (NAnosecond GIgawatt RAdar), was recently built by the Russians for Marconi (10 GHz, 0.5 GW, 5 ns, 150 Hz, 3° beam width), and installed at a test site on the South coast of the United Kingdom (see Fig. 21).[102] It uses numerical MTI (moving-target indicator) algorithms to provide 30 dB suppression of echoes from stationary targets and 10–20 dB suppression of echoes from windblown vegetation and sea clutter. In joint Russian–Marconi experiments, moving targets of $\sim 1\ \mathrm{m}^2$ radar cross section were reliably tracked at distances up to 100 km over the sea and wood-covered terrain, and near 1-m range resolution provided identification of targets and measurement of target parameters. In particular, the rotation of a helicopter's blades could be clearly seen.

FIG. 21. Photograph of a nanosecond radar system. (Reproduced with the permission of GEC-Marconi and the United Kingdom Ministry of Defense.)

2. Millimeter-wave radars

The gain of an antenna is limited to $G < \pi^2 D^2/\lambda^2$, where D is the antenna diameter. Shortening the wavelength allows one to greatly increase the antenna gain for a fixed antenna size, or alternatively to use more compact antennas to achieve the required gain. There are a variety of tradeoffs in choosing the optimum operating frequency of a radar system, including directionality, resolution, Doppler sensitivity, atmospheric attenuation, and the effective cross section of the scattering objects. The potential advantages of millimeter-wave radars over lower frequency systems include smaller antennas, narrower beam widths, greater Doppler sensitivity, lower vulnerability to jamming or intercept, reduced clutter and multipath effects, and higher precision target location. There are at least two areas in which high-power millimeter-wave radars can be strongly advantageous: active monitoring of the atmosphere and the search for debris in space.

The active monitoring of the atmosphere by millimeter-wave radars makes it possible to study the dynamics of clouds and to resolve multiple cloud layers, which is important for meteorology and the study of global warming.[103,104] (Note that the effect of clouds on global warming can be at least as significant as that of greenhouse gases.[105]) The advantage of millimeter waves for these applications is their ability to propagate well through particulates, and at the same time to scatter off them strongly enough for detection. The scattering is in the Rayleigh regime, and scales as D^6/λ^4, where D is the diameter of the aerosol and λ is the radiation wavelength. Because of this scaling, scattering of

longer-wavelength microwaves is not detectable. On the other hand, visible or near-infrared radiation from lasers scatters so strongly that objects such as clouds are opaque.

A number of atmospheric studies of clouds and thunderstorms were done at millimeter wavelengths using low-power sources (extended-interaction oscillators with a few watts of average power).[106] However, low-power sources restrict the radar range (particularly in humid air), limiting it to near-vertical operation, and also limit its use to strongly reflective cloud layers. By increasing the average transmitter power by three orders of magnitude, a 94-GHz radar system could overcome an additional 30 dB of atmospheric absorption, which would increase the useful range by at least 15 km (in the most humid conditions). This would allow the probing of cloud layers at a wider range of angles extending to near horizontal. One of the first results obtained with a high-power millimeter-wave radar was the detection of a scattered signal from apparently clear air at a range of a few hundred meters by using a 10-kW (cw) 84-GHz gyrotron in a bistatic configuration.[107]

Conventional radars generate phase stable, carefully tailored microwave pulses at low power, and then use a power amplifier to generate the required radiated signal level. Advances in the millimeter-wave radars are thus related to advances in millimeter-wave amplifier tubes, and in particular to the development of gyroklystrons. During the last decade, the IAP, in collaboration with the Russian company ''Toriy,'' developed a 35-GHz gyroklystron (GKL) producing 750 kW in 100-μs pulses at 5 Hz repetition rate.[108] At 94 GHz, an IAP collaboration with the Russian company ''Istok'' developed a GKL with 65 kW output power and 0.3% bandwidth.[109] Recently, a similar tube was built at NRL. This tube delivered 67 kW with an improved 0.5% bandwidth.[110]

The progress in the development of high-power GKLs has led to the suggestion to build a 35-GHz radar capable of detecting small-size orbital debris that is dangerous for spacecraft and space stations. Such a radar was first suggested in Ref. 111 and then described in Ref. 97. According to the estimates given in these references, approximately 20 MW of power is required to detect a 1-cm object at a range of 1000 km using a 20-m tracking antenna. At the current state-of-the-art, 30 GKLs feeding a large phased-array antenna could be used for such a radar system. Such a radar is capable of two regimes of operation, using slow mechanical and fast electronic steering: a seeking regime with a large angular divergence of the radar beam, and a tracking regime in which the angular divergence of the radar beam is only $\sim 10^{-3}$ rad. Four such stations, distributed along the Earth's equator, would be enough to catalog orbital debris larger than 1 cm.

3. Gyroamplifiers for communications systems

For communications systems, high-power broadband gyro-traveling-wave tubes (gyro-TWTs) are of great interest. However, early attempts at building such amplifier tubes were plagued by oscillation due to both absolute and convective instabilities. In recent years, a better understanding of these instabilities, and how to avoid them, has allowed considerable experimental progress to be made. At NRL, a two-stage tapered gyro-TWT was developed for operation in the vicinity of 35 GHz.[112] This device used a downtapered rectangular input waveguide, followed by a cutoff drift section and an uptapered output waveguide. It demonstrated 20% instantaneous bandwidth (32–39 GHz), 8 kW of output power at an efficiency of 16%, and a saturated gain of 25 dB. A peak output power of 10 kW was observed at 33 keV, 2 A. At the National Tsing Hua University (Taiwan), a 34-GHz gyro-TWT demonstrated 33 dB of gain, an instantaneous bandwidth of 12%, and a power level of 62 kW with 21% efficiency, using a 100-keV, 3-A electron beam.[113] (They recently reported an increase in the gain to 50 dB with 10% bandwidth.[114]) The gain-bandwidth product in these tubes is several times larger than that of a conventional TWT in this frequency band. At lower frequencies (15.3 GHz), the successful operation of a single-stage gyro-TWT at the second cyclotron harmonic was demonstrated at the University of California at Davis.[115] In this experiment, an 80-keV, 20-A electron beam produced over 200 kW of microwave power with $\sim$13% efficiency, large-signal gain of 16 dB, and saturated bandwidth of 2.1%. These sources are also relevant to military jammers and electronic warfare systems.

D. High-peak power sources

The last category that we treat in this review is the high-peak power, generally single-shot microwave source. Such sources are often developed to explore new device concepts or new physics, or to explore the ultrahigh power limit of sources driven by large pulsed-power drivers. An important application of these sources has been to develop microwave ''simulators,'' that is, microwave sources designed to test the possible effect of intense microwave pulses on electronic systems. In addition to peak power, another important figure of merit for high-peak power sources is the energy contained in a single pulse. One of the goals has been to develop sources that can produce 1 kJ of microwave energy in a 1-μs pulse, requiring an average power of 1 GW through the pulse. Virtually all ultrahigh-peak power sources suffer from pulse shortening, as discussed in Sec. III, so that a 1-μs pulse is typically not achievable, even if a long-pulse electron beam can be generated. As a result, only a few high-voltage source technologies have approached the 1 kJ single-pulse energy level.

Before presenting results from this category of devices, it is worth noting that the standards of accuracy and precision in high-peak power, single-shot experiments are necessarily different from that of high-average power, repetitively pulsed devices. For repetitively pulsed devices, average power is almost always measured calorimetrically, leaving little room for error. In addition, the frequency spectrum can be measured to high precision using frequency counters and spectrum analyzers, and very precise measurements can be made of device performance, since for a given set of experimental parameters, every pulse is virtually identical. However, most single-shot power measurements are performed by less certain means. For power measurements, it is typical to use directional couplers, or microwave pickups in the far

field of highly overmoded antennas, followed by many tens of dB of microwave attenuation before detection of the microwave signals at the mW level using crystal detectors. Often, the frequency spectrum is broad, with side lobes or multiple modes excited, but frequency diagnosis may be limited to the use of discrete bandpass filters. Often, the geometry is highly overmoded, making it difficult to carry out precise calibrations. Often, the data set is limited, and exhibits substantial shot-to-shot variation, making it difficult to perform meaningful averages. (In fact, the highest single-shot power measurements are sometimes reported, since every shot is in essence a separate experiment.) Even with careful calibration, 3 dB (i.e., factor of 2) error bars are typical. Nevertheless, despite these experimental difficulties, a large variety of impressive results have been documented. In addition, there have been some recent improvements in diagnostic procedures, including the increased use of heterodyne techniques for single-shot spectral measurements, and of oscilloscopes that can capture and display transient wave forms at frequencies up to 10 GHz.

1. Vircators

Vircators have been a popular research area because they are the simplest method of generating microwave radiation from an intense relativistic electron beam. They have the virtue of being extremely low-impedance devices and can thus utilize ultrahigh-current electron beams to reach very high peak powers. They can also operate in extremely low quality factor ($Q \sim 1-10$) cavities, or even without a well-defined cavity structure. However, they are generally not highly efficient devices. In addition, since the amplitude and frequency of electron oscillations are restricted by the breakdown limit, and because of problems with plasma expansion, most vircator experiments have operated at relatively low frequencies ($\lesssim 3$ GHz) and for short pulse lengths. Moreover, they cannot be operated in an amplifier configuration, although phase-locked vircator oscillators have been reported. In recent years, vircator experiments have been aimed at several goals: improving the efficiency, reducing the linewidth or phase locking the output, increasing the peak power, increasing the operating frequency, and increasing the pulse length (which is normally limited by rf breakdown). The efforts to improve the coherence and efficiency of vircators have included putting various resonant cavity structures around the virtual cathode. Because vircators can be very low-impedance devices, they are a candidate device for operation using an explosive driver. These and other issues important for vircators are discussed in more details in Refs. 1, 116, and 117. The early vircator experiments are reviewed in Refs. 118 and 119. We present some of the recent high-power experimental results in this section.

Davis *et al.* carried out a reditron experiment that produced 1.6 GW in a 30-ns pulse at 2.46 GHz with $\sim 6\%$ efficiency, using a 1.3-MeV, 22.5-kA electron beam.[120] Hwang and Wu report a 1.4 GW vircator experiment, carried out jointly between the Taiwan Institute of Nuclear Energy and the National Tsing Hua University, with a dominant frequency of 8.2 GHz, that operated at 6% efficiency in a ~ 20-ns output pulse.[121] Sze *et al.* phase locked two 300-MW, 2.8-GHz vircators, using a microwave signal from a relativistic magnetron.[122] A single high-voltage pulse drove the magnetron and both vircators in that experiment. These three experiments were driven by pulse line accelerators. Azarkevich *et al.* report a vircator powered by an explosively driven magnetocumulative generator using 200–600 g of chemical explosive. It operated at voltages up to 600 kV and currents up to 16 kA, producing ~ 100 MW at ~ 3 GHz with a microwave pulse of 100–200 ns.[123]

The highest power conventional pulsed-power system known to have been used for a microwave generation experiment was Aurora, a large nuclear-weapons-effect bremsstrahlung generator that was located at the Harry Diamond Laboratories near Washington, DC until its decommissioning in 1995. It had four parallel Blumlein pulsers, each of which could produce a 10-MeV, 250-kA, 180-ns pulse into an $\sim 35\ \Omega$ load. A set of vircator experiments were carried out using one arm of Aurora. These experiments reported ~ 400 J in $\sim 100-150$-ns broadband microwave bursts at frequencies below 1 GHz, or 4 GW averaged over the pulse length, corresponding to an efficiency of a few tenths of 1%, based on typical beam parameters of 6.5 MeV and 300 kA, with still higher instantaneous powers observed within the pulse.[124]

2. Relativistic klystron oscillators and amplifiers

Research on klystrons driven by intense relativistic electron beams began in the early 1970's with the work of Friedman at NRL, who studied automodulation of an intense relativistic electron beam passing through a set of cavities in a cylindrical drift tube and then devised a means to extract microwave power from the modulated beam into an output waveguide.[13] These early experiments produced ~ 600 MW at ~ 2.9 GHz with 20% efficiency, using a 400-keV, 6-kA beam from an explosive-emission diode driven by a pulse line accelerator. Later, Friedman and co-workers demonstrated that the automodulation was due to reflexing electrons caused by virtual-cathode formation in the cavities,[12] with the intense-beam physics seen in the vircator used here to create the same feedback mechanism as in an ordinary reflex klystron (see Ref. 125), and the device became known as a relativistic klystron oscillator (RKO). Lowering the beam current below the threshold for virtual-cathode formation, in order to suppress the oscillation, and driving the first cavity with an external microwave signal, created the first intense beam, or high-perveance relativistic klystron amplifier (RKA), which produced ~ 3 GW at 1.3 GHz with ~ 40 dB gain and $\sim 40\%$ efficiency.[126] Even in these amplifier experiments, space charge dominates the bunching process, and very effective bunching can be obtained in a single cavity, as discussed in Sec. II. The NRL work has produced a number of impressive results. One recent RKA experiment produced 2.85 ± 0.15 GW at 1.28 GHz with $\sim 60\%$ instantaneous efficiency, using a 450-keV, 11-kA beam with a 130-ns voltage flat top.[127] This experiment made use of inductively loaded rf gaps, eliminating the space-charge depression normally seen in RKA gaps, and was noteworthy in that no sign of pulse shortening was observed in the rf pulse, resulting in an overall $\sim 50\%$ energy efficiency. An earlier

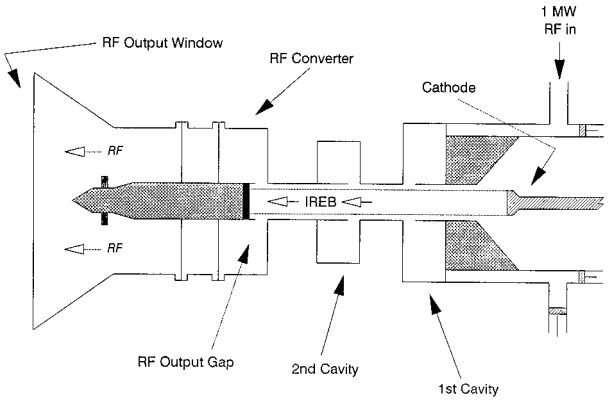

FIG. 22. Schematic diagram of the 15-GW, 1.3-GHz relativistic klystron (after Ref. 128).

NRL experiment, illustrated in Fig. 22, produced ~15 GW at 1.3 GHz, with a single-pulse energy of 1.3 kJ.[128] This seems to be the only high-peak power HPM device that has clearly exceeded 1 kJ in single-pulse energy. This technology is now being extended to the *X* band, and a triaxial RKA at NRL has already achieved full modulation of a 400-keV, 16-kA electron beam at 9.6 GHz, with microwave extraction experiments planned in the near future.[129]

RKA and RKO experiments have been carried out at a number of other laboratories. Hendricks *et al.* at the Air Force Phillips Laboratory reported an injection-locked 1 GW RKO at 1.3 GHz that operated at ~20% efficiency in pulses of up to 200 ns,[130] using a 500-keV, 10-kA, 300-ns electron beam. Levine and Harteneck at Physics International Corporation reported a repetitively pulsed RKA that produced 250–300 MW peak power at 1.3 GHz in 80-ns pulses at repetition rates of up to 200 Hz.[131] Fazio *et al.* at Los Alamos National Laboratory reported a 500-MW, 1.3-GHz RKA with a FWHM of 0.5 μs, using a 600-keV, 5-kA electron beam.[132]

The ''super-reltron'' is a klystron-like variant of the conventional vircator that was developed by Titan Advanced Innovative Technologies of Albuquerque, NM (see Fig. 23). In this device, a modulated electron beam is generated by periodic virtual-cathode formation in a modulating cavity, the modulated beam is postaccelerated to reduce the relative energy spread, and finally a multicavity output section is used to extract the beam kinetic energy. These devices have produced 600 MW at 1 GHz in a 0.5–1-μs pulse with 40% efficiency, using an injector voltage of 250 kV, a current of 1.35 kA, and an accelerating gap voltage of 850 kV; and 350 MW at 3 GHz with 37% efficiency, using a 200 kV injector, 1-kA beam, and 750 kV postacceleration.[133] One version of their 3-GHz tube was tunable by ~5% by mechanically varying the resonant frequency of their modulating cavity.

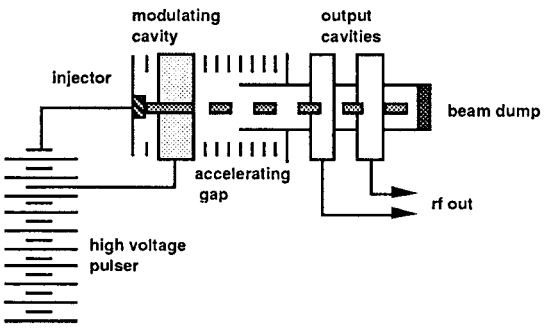

FIG. 23. Schematic of a Super-Reltron (after Ref. 133).

3. Relativistic BWOs, TWTs, and related devices

In backward-wave oscillators (BWOs), the wave energy propagates counter to the direction of electron flow, as discussed in Sec. II. This internal feedback mechanism makes it possible to excite oscillations over a wide range of beam parameters, making these devices relatively insensitive to electron velocity spread. This is one reason why the first successful experiments aimed at efficient, high-power microwave generation from relativistic electron beams were carried out with BWOs.[134–136] Later, more complicated versions of BWOs were studied for power and efficiency enhancement.

One of the ways to increase the BWO power is to operate in higher order modes using tubes with enlarged cross sections. However, to do this successfully, it is necessary to avoid exciting parasitic modes with frequencies close to the operating mode. One unique method of doing this is to damp the parasitic modes by means of cyclotron-resonant absorption of their radiation. However, the electron-beam radius should correspond to a null in the coupling of the cyclotron wave to the zeroth spatial harmonic of the operating mode, in order to avoid also suppressing this mode. This idea was successfully realized in a BWO experiment in which the parasitic TM_{12} mode was suppressed by cyclotron absorption, while the operating TM_{02} mode was stably excited, producing 1.6 GW at 7.5 GHz with an efficiency of ~10% from a 1.3-MeV, 10-kA electron beam.[137]

Two ideas have been suggested to enhance the efficiency of BWOs. The first is based on increasing the coupling impedance to the wave in the output portion of the slow-wave structure, in order to compensate for the unfavorable axial structure of a backward wave, which is largest near the beam entrance and near zero at the exit.[138] By changing the amplitude of the ripples [see Fig. 1(a)] in order to increase the coupling impedance near the end of the slow-wave structure, the efficiency of an *X*-band BWO driven by a 500-keV, 6-kA electron beam was increased from the 10%–15% typical of simple BWOs to ~35%, resulting in an output of ~1 GW in short (1.5–2 ns) pulses.[139]

The second idea is based on axially profiling the phase velocity of the backward wave, which is similar to the tapering discussed in Sec. II for FELs and CRMs. To realize this, a slow-wave structure consisting of two parts with different periods was used. In experiments carried out at the Institute of High Current Electronics (IHCE) in Tomsk, Russia, the efficiency of a BWO driven by a 400-keV, 2.8-kA beam was increased to 45%, producing 500 MW at 9.4 GHz.[140] Later, a similar experiment was performed at the University of New Mexico (UNM) in collaboration with members of the IHCE team, producing 550 MW at 9.45 GHz in an 8-ns pulse from a two-stage BWO driven by a 620-keV, 5.2-kA electron beam.[26]

TABLE V. Relativistic BWOs, TWTs, and related devices.

Type of device	Laboratory	V (MeV)	I (kA)	P (GW)	η (%)	f (GHz)	Ref. No.
BWO	IAP	1.3	10	1.6	10	7.5	137
BWO	IAP/IHCE	0.5	6	~1.0	35	10	139
BWO	IHCE	0.4	2.8	0.5	45	9.4	140
BWO	UNM/IHCE	0.62	5.2	0.55	~20	9.45	26
TWT	IAP	0.35–0.65	1.5–2.0	0.1	~10	36	141
TWT	Cornell U.	0.85/	~1.0/	0.4/0.16	45/	10	142,143
MWCG	IHCE	2.1	15	15	~50	10	144
MWCG	IHCE	1.2	12	3	~20	30	144
RDG[a]	IHCE	1.6	17	4.5/(9)	15/(30)	~30	144
RDG[a]	IHCE	1.5	16	3.5/(7)	15/(30)	45	144

[a]Power and efficiency in parentheses refer to power at output of generator, before radiation into the atmosphere.

For high gain, efficient, stable operation of TWT amplifiers, the key issue is to avoid self-excitation of backward waves. One means to discriminate against these waves is to divide the interaction space into two sections separated by a sever made from lossy material. In experiments at the IAP, such a two-stage TWT produced 100 MW at 36 GHz with an efficiency of 8%–11%, and gains of 48 and 44 dB, respectively, in the small and large signal regimes.[141] In experiments at Cornell University, Nation and co-workers produced 400 MW in the *X* band with 45% efficiency at a gain of 37 dB.[142] However, the spectrum of radiation was 300-MHz wide, and up to half of the power was in side bands. Later, the same group carried out an experiment in which 160 MW was produced at ~9 GHz with a spectrum of <50 MHz.[143] Their single-shot, cold-cathode experiments are intended to point the way to high-power amplifiers for future linear colliders.

Relativistic diffraction generators (RDGs) and multiwave Cherenkov generators (MWCGs) are another group of HPM sources based on Cherenkov radiation. In these devices, an annular relativistic electron beam passes through a pair of rippled-wall sections in overmoded cylindrical waveguide and interacts either with volume or surface waves of the structure. These devices have a close relationship to BWOs and TWTs, but their operation is more complex, due to their highly overmoded nature. According to Ref. 144, MWCGs have produced 15 GW in a 60–70-ns pulse at ~10 GHz with a 2.1-MeV, 15-kA beam at an efficiency of ~50% and 3 GW in a 70-ns pulse at ~30 GHz with a 1.2-MeV, 12-kA beam at ~20% efficiency. RDG experiments have reported 4.5 GW of radiated power (9 GW of power at the antenna feed) at ~30 GHz using a 1.6-MeV, 17-kA beam at 30% electronic efficiency, and 3.5 GW of radiated power (7 GW of power at the antenna feed) at ~45 GHz using a 1.5-MeV, 16-kA electron beam, also at 30% electronic efficiency.[144] Pulse lengths of up to 700 ns are reported for the 45-GHz experiment at 2.8 ± 0.8 GW of power, for a pulse energy of 520 J.

All these results are summarized in Table V.

Before concluding this section, let us briefly discuss the effect of plasma filling on the operation of HPM sources. One of the obvious benefits of introducing a plasma is the neutralization of space-charge effects in high-current electron beams. A number of experiments with currents several times larger than the vacuum space-charge limiting current [see Eq. (20)] were successfully carried out with plasma-filled relativistic BWOs[145] and gyrotrons.[146] It was even reported that the addition of a background plasma into a relativistic BWO resulted in an eightfold increase in its efficiency, producing a peak power of ~450 MW at 8.4 GHz from a BWO driven by a 630-keV, 2.3-kA electron beam.[147] Let us also mention the work of Strelkov and co-workers at the Institute of General Physics in Moscow, in which a hollow 540 kV, 2.4-kA electron beam propagating in a smooth-wall metal drift tube was enclosed by an annular plasma layer which played the role of a dielectric to support slow waves.[148] In this plasma Cherenkov device, ~85 MW of broadband radiation in the frequency range 3–32 GHz was produced at 7% efficiency. One key to this experiment was the use of a relativistic electron beam to excite plasma waves with large group velocities; these waves couple well to the modes of a vacuum waveguide, making it possible to extract the power from the plasma region into free space.

4. Relativistic magnetrons

The magnetron is another device that has been extrapolated with great success to high-peak power, short-pulse operation, particularly at the lower microwave frequencies. The first significant relativistic magnetron experiment was carried out by Bekefi and co-workers in 1976. That experiment produced 1.7 GW at 3 GHz in a 30-ns pulse with 35% efficiency.[149] Other high-peak power experiments were carried out by groups in the FSU and the U.S. In the FSU, a set of experiments were carried out in the *X* band. In order to prevent damage to the vanes of the anode structure, the diffraction coupling scheme discussed in Sec. II was employed, in which the electrons propagate along with the microwave radiation through the output end of the device [see Fig. 2(b)]. This allowed Kovalev and co-workers to produce 4 GW at 9.2 GHz.[150] Much of the recent work in this area has been carried out at the Physics International Company. In 1985, Benford *et al.* developed a 6.9-GW, 4.5-GHz magnetron.[151] More recently, this group studied phase locking and high-repetition rate operation. Levine *et al.* reported phase locking an array of seven relativistic magnetrons, producing 2.9 GW at 2.8 GHz, and burst-mode operation of 400–600 MW, 75-ns relativistic magnetrons in the frequency range of 1–3

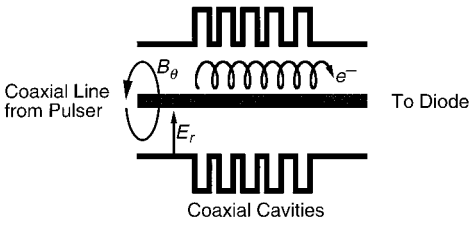

FIG. 24. Schematic diagram of a MILO.

GHz at up to 100 Hz for 10 s.[152] Levine and co-workers also reported the development of tunable magnetrons, demonstrating a 24% tuning range about a center frequency of 1.21 GHz in a 400 MW magnetron, and a 33% tuning range about a center frequency of 2.82 GHz in a 500 MW magnetron.[153]

The MILO (magnetically insulated line oscillator) is a cross-field oscillator in which the required magnetic field is supplied by the electron-beam current, rather than by a separate magnet. In the MILO configuration (see Fig. 24), a set of coaxial resonators is attached to the outerwall of a cylindrical transmission line enclosing the cathode stalk. When a negative voltage pulse is applied, explosive electron emission from the cathode is radially confined by the magnetic field (magnetic insulation), so that the electrons are forced to flow parallel to the axis of the device. However, as in the relativistic magnetron, electrons undergo cross-field drift and some are deposited on the slow-wave structure, generally leading to plasma generation and pulse shortening. Recent MILO experiments operating at ~ 525 kV have reported powers >1 GW near 1 GHz with pulse lengths <100 ns. The experimental efficiency has approached 5%.[154]

5. Relativistic gyrodevices

Thermionic gyrotron oscillators have proved to be efficient sources of high-power microwave radiation and offer easy scaling to millimeter wave, and even to submillimeter wave, frequencies. This high-frequency advantage, compared to slow-wave devices, persists at higher voltage, even though the required magnetic fields scale upwards with γ.

Studies of the gyrotron interaction using pulse line accelerators began in the 1970's. Among the initial studies was one using a 3.3-MeV pulser to produce microwave peak powers of approximately 1 GW at 8 GHz; however, no resonant cavity was employed in that experiment, and the device produced microwaves with an efficiency of $<1\%$.[155] Subsequent studies employing resonant cavities were carried out primarily in the FSU, often employing 350-keV, $\sim$1-kA electron beams. Among the results were 25 MW at ~ 10 GHz with 20% efficiency,[156] and 23 MW at 40 GHz with 5% efficiency.[157] In addition, 60 MW was produced at 15% efficiency in a plasma-filled gyrotron that operated above the vacuum space-charge limited current.[146] Following this, a series of experiments was carried out at NRL between 1984 and 1989 that explored high-peak power gyrotron operation at 35 GHz and higher frequencies. In the NRL experiments, the beam transverse momentum was supplied by sending the electron beam through a nonadiabatic dip in the magnetic field produced by a ''kicker'' magnet. A number of experiments were carried out at voltages of up to 800 kV and currents up to 1.6 kA using a compact Febetron pulser.[158] These experiments produced 100 MW at 35 GHz with 8% efficiency in the TE_{62} mode, and demonstrated high-power operation at frequencies ranging from 28 to 49 GHz by magnetically tuning through a family of TE_{m2} modes. The final experiment in this series operated on the much larger VEBA pulser at 1–1.35 MV and 2.5 kA, and produced 275 MW at 35 GHz in a 40-ns pulse with 14% efficiency.[159]

Work on pulsed-power-driven gyrodevices, in particular the gyro-backward-wave oscillator (gyro-BWO) configuration, has been under way at the University of Michigan for the past decade. A recent paper reports 11 MW of extracted power in the frequency range 3.2–6 GHz from a gyro-BWO with a tapered axial magnetic field and operating at 700–900 kV with a 1–4-kA beam.[160] Related work is also under way at the Phillips Laboratory.[161] NRL has explored gyroklystron[162] and gyro-traveling-wave amplifier configurations[163] driven by pulse line accelerators. The latter experiment demonstrated 30 dB of gain at 35 GHz, and produced 20 MW at 11% efficiency in a circularly polarized TE_{11} mode, using a 900-keV, 300-A low-velocity spread electron beam produced from an explosive-emission gun using a beam scraper as an emittance filter, and followed by a short bifilar helical wiggler magnet to produce the required transverse momentum. This gyro-TWA operated near ''grazing intersection'' between the dispersion curves for the beam and waveguide modes, where the upper (CARM) intersection and the lower (gyrotron) intersection merge, and could also have been considered a CARM amplifier, since the operating frequency was 4.4 times the relativistic cyclotron frequency. More recently, Menninger *et al.* at MIT reported 4 MW at 17.1 GHz in a 20-ns output pulse at 6.5% efficiency, with 51 dB of gain, from a gyro-TWT that operated in the third cyclotron harmonic, using a 380-keV, 160-A electron beam from a thermionic electron gun driven by an induction accelerator.[164]

Unlike the gyrotron, the frequency of the cyclotron autoresonance maser (CARM) scales upwards in frequency as the voltage is increased, since the relativistic frequency upshift ($\sim\gamma^2$) more than cancels the relativistic decrease of the electron gyrofrequency (γ^{-1}), producing an overall γ scaling of the output frequency. However, like FELs and unlike gyrotrons, the presence of the Doppler term in the resonance condition makes CARM devices very sensitive to spreads in electron axial velocity (though they are insensitive to spreads in electron energy). Since the production of high-transverse-momentum electron beams ($\beta_\perp \sim \gamma^{-1}$ is close to optimum) generally increases the axial velocity spread, CARM devices, both hot cathode and cold cathode, have generally fallen far short of their theoretical cold-beam efficiencies. The results of CARM experiments during the 1980's were presented in Ref. 165. Below we will review the recent results.

DiRienzo *et al.* reported a 35-GHz CARM amplifier powered by a 1.5-MeV, 130-A, 30-ns electron beam from an explosive-emission electron gun. Like the NRL gyro-TWA, this experiment used an emittance selector to produce a low-velocity-spread electron beam, followed by a short bifilar wiggler magnet to produce the required transverse momen-

tum. This experiment produced 12 MW at 6.3% efficiency with an input power of 17 kW, and demonstrated a linear growth rate of 50 dB/m.[166] In a recent second-harmonic cold-cathode CARM oscillator experiment, Cooke *et al.* reported 170 kW at 14.27 GHz at 3.9% efficiency, using a 14-A, 300-keV electron beam at a magnetic field of 2.17 kG.[167] In this case, the output frequency was 3.7 times the relativistic cyclotron frequency. However, the most impressive recent CARM results were reported from a cold-cathode oscillator experiment at the IAP that made use of extensive beam scraping to produce a 100-A, 500-keV low-velocity-spread linear electron beam. The low-velocity-spread in this device was preserved as the transverse momentum was increased to $\beta_\perp \sim 0.55$ by a properly designed and fabricated kicker magnet. This experiment reported 13 MW at 38 GHz in a ~ 6-ns FWHM pulse at an efficiency of 26%,[168] using a 12.4-kG magnetic field and a Bragg-resonator cavity. The theoretical efficiency in this case was $\sim 30\%$, and the relativistic cyclotron frequency in this case was 17 GHz, indicating a frequency upshift of ~ 2.2.

6. Free-electron lasers and masers

The term ''free-electron laser,'' or ''FEL,'' is generally used to describe devices that generate coherent radiation (''light'') by means of a fast-wave interaction in which a beam of relativistic ''free'' electrons is induced to radiate coherently by passage through a periodic wiggler field, and this is the definition we use here. However, it is worth noting that the term does not apply uniquely to fast-wave devices, and does not refer directly to a particular radiation mechanism or specifically to bremsstrahlung devices. For that reason, any source of coherent electromagnetic radiation in which the active medium is a beam of electrons might be referred to as a FEL. For instance, Cherenkov devices are sometimes referred to as Cherenkov FELs. In the microwave and millimeter-wave portions of the spectrum, FELs are also known as free-electron masers (FEMs) or ubitrons. We will refer to these devices generically as long-wavelength FELs, to distinguish them from the higher voltage optical FELs that can produce radiation through the IR, visible, and UV portions of the electromagnetic spectrum.

The history of long-wavelength FEL research began with the thermionic ubitron experiments of Phillips in the 1960's.[169] In the 1970's, attempts were made to extend this work to high-peak-power levels using intense relativistic electron beams from field-emission diodes driven by pulse line accelerators. The efficiency of these early pulsed-power FEL experiments was typically $\ll 1\%$, due principally to the use of beams with excessively large velocity spreads, although one early experiment reported 30 MW at ~ 10 GHz with $\sim 5\%$ efficiency from a FEL oscillator driven by a 700 kV electron beam.[170] The history of these early FEL experiments is described in Refs. 171 and 172. The first breakthrough in efficiency in a millimeter-wave FEL came in an experiment at NRL that used a beam-scraper diode to form a 1.35-MeV, 1.5-kA low emittance electron beam, and generated 35 MW at ~ 70 GHz with 2.5% efficiency in a superradiant amplifier configuration.[173] Later experiments in this series increased the efficiency to 6% using a tapered axial magnetic field, one of several known techniques for increasing FEL efficiency by tapering the interaction parameters, and demonstrated high-gain amplifier operation (50 dB total gain at 1.2 dB/cm) at 35 GHz.[174] Later, at somewhat higher voltages, the ELF (Electron Laser Facility) project at LLNL produced >1 GW at 35 GHz in a 20-ns pulse with a FEL amplifier driven by a 3.5-MeV, 850-A electron beam from the ETA induction linac in which the strength of the wiggler magnetic field was tapered to produce an efficiency of 34%.[175] A later experiment in that series produced 1–2 GW at 140 GHz in a 20-ns pulse, using a ~ 6-MeV, ~ 2.5-kA electron beam from the ETA-II accelerator.[176] This 140-GHz FEL was developed for a tokamak heating experiment. A major breakthrough in efficiency in an untapered FEL was reported by Conde and Bekefi, using a reversed guide magnetic field, in which the sense of electron gyration in the axial magnetic field was opposite to the direction of the circularly polarized wiggler magnetic field. This experiment used a 750-keV, 300-A electron beam to produce 61 MW at 33 GHz with 27% efficiency.[177]

Long-wavelength FEL research has been carried out at many institutions around the world in recent years, and has been aimed at achieving high efficiency, higher frequencies, broad amplification bandwidths, and more compact systems. Bratman *et al.* report a tunable FEM oscillator that generated 7 MW at 45 GHz at 12% efficiency, using a 500-keV, 120-A, 20-ns electron beam.[178] Cheng *et al.* report a millimeter-wave FEL using a short-period (9.6 mm) wiggler and a sheet electron beam that produced 250 kW at 86 GHz with 24 dB of gain and $\sim 3\%$ electronic efficiency. The 450-keV, 17-A sheet electron beam was produced from a rectangular cold cathode by means of substantial beam scraping in a double-anode structure.[179] Saito *et al.* reported an *X*-band FEL that produced 120 MW at 9.4 GHz, using a 1.5-MeV, 700-A electron beam from an induction linac.[180] Kaminsky *et al.* report a Bragg-resonator FEL oscillator driven by a 1-MeV, 200-A, 200-ns electron beam from an induction linac that produced 23 MW at 31 GHz with 19% efficiency in the reversed-guide-magnetic-field regime.[181] Agafonov *et al.* report a FEM oscillator driven by a 1-MeV, 1.5–3-kA, 5-μs sheet electron beam that produced tens of MW of millimeter-wave radiation (total energy ~ 200 J), mostly in the vicinity of 4 mm, in a 3-μs pulse at an efficiency of $\sim 4\%$ efficiency.[182] In superradiant experiments by the same group, powers as high as 300 MW were observed (calorimetrically) in the wavelength range 2–15 mm.

V. SUMMARY

Our intention in writing this article has been to provide an introduction to some of the concepts, issues, technologies, and research activities in high-power microwave generation research. Dramatic advances have been made in both high-peak and high-average power microwave sources over the past decade, as we have outlined above. However, this field has by no means reached its limits. New high-power sources will be needed for future fusion devices, future accelerators, and future military systems, including radar and electronic warfare devices. There are also other potential applications, in addition to those mentioned above, such as material processing and atmospheric modification. Material pro-

cessing now uses gyrotron technology originally developed for the fusion program to provide high average power millimeter-wave radiation for ceramic sintering and other applications.[183] Microwave atmospheric modification includes a possible solution to such global problems as ozone depletion and global warming,[184] which would require major advances in HPM source technology, as well as to such local problems as the removal of halocarbons from air in the vicinity of industrial plants following accidental leakage,[185] which might use high-power sources already developed for fusion and other applications. For these reasons, HPM research continues at a large number of research institutions in the U.S. and around the world.

Looking ahead, the best way to predict future progress in high-power microwave source development is by observing where improved sources are needed, and where research efforts are currently under way. The fusion application has motivated a great deal of progress in the development of millimeter-wave gyrotrons capable of megawatt power levels with more than 1 MJ of energy in a single pulse. Nevertheless, this application still requires a further significant increase in microwave pulse duration. The most important obstacle in this path is the problem of controlling the temperature of the output window. One promising new technology is the use of artificial diamonds as windows,[186,187] whose improved thermal conductivity and lower microwave absorption may finally allow a true cw megawatt or even multimegawatt gyrotron oscillator to be developed.

In the area of sources for accelerators, near-term research seems likely to push the power of *X*-band klystrons past 100 MW in microsecond-length pulses, and research is continuing on *X*-band sources, such as the magnicon, that have the potential to exceed 60% efficiency. There is also a major effort to push the art of high-power amplifier tubes to higher frequencies, such as 34 GHz, for proposed future multi-TeV colliders, with a long-range goal of 100 MW sources with an efficiency greater than 40%. While conventional relativistic klystrons have made the fourfold leap in frequency from *S* band (2.856 GHz) to *X* band (11.424 GHz), it seems likely that new technologies will be required at 34 GHz and beyond, and possibilities include multibeam or sheet-beam klystrons, gyroklystrons, magnicons, and ubitrons, all of which are proposed or currently under investigation.[62]

In the area of sources for radar and communications, work is now in progress to improve the average power of gyroklystron amplifiers at 94 GHz in order to build tubes suitable for use in future radar systems, and there will probably be an attempt to improve the bandwidth of these tubes beyond 1 GHz, perhaps by investigating gyrotwystron or gyro-TWT configurations.

In the area of high peak power sources, there are already commercial products available from a number of suppliers, including repetitively pulsed magnetrons, vircators, BWOs, super-reltrons, and RKAs, but the market for these sources is presently limited to research applications. It seems likely that the present research focus on the problem of pulse shortening will lead to improvements in single-shot microwave energy beyond the 1 kJ level, and that the increased application of technology from the microwave tube industry will lead to HPM tubes with longer lives and higher average powers. However, practical applications for such sources seem to be somewhere in the future.

The rate of progress in all of these areas depends critically on the cycles of research interest and funding. In the U.S., for instance, research on fusion-class gyrotron oscillators has fallen substantially in the past few years, due to cutbacks in the overall Department of Energy (DoE) magnetic fusion research program. However, DoE support of microwave amplifier research for future linear colliders has remained strong, and new high-power tubes may be required for the proposed tritium-breeding high-average power proton accelerators known as APT. In the Department of Defense (DoD), there has been continued funding of high-peak power microwave sources as well as a recent interest in gyroamplifiers for millimeter-wave radar systems. In Russia, the government support has fallen for some purely scientific projects, such as accelerator-class 14-GHz klystrons, but research continues in the development of gyrotrons for ITER and other controlled fusion reactors, or with potential commercial or military applications, such as to material processing or radar systems. It seems safe to assume that, while particular areas of research will respond to changing interests and opportunities, overall interest in HPM generation of research will remain strong for many years to come.

This article has included only a fraction of the interesting and important recent results on HPM generators, and should be considered only as an introduction to this exciting field of research. More detailed information on source research and applications is available from a variety of sources. There are several recent books, including Refs. 58, 188, and 189. High-power microwave systems and effects are discussed in Ref. 190. The most popular place to publish new results in high-power microwave generation research has been a series of biennial Special Issues on High-Power Microwave Generation of the IEEE Transactions on Plasma Science. The most recent of these was published in June 1996,[191] and the next is scheduled for June 1998. There are also a number of conferences that deal specifically with this research area; their proceedings are useful references to current research in the field. Developments in high-peak power (as well as high-average power) microwave source research are the subject of a series of annual SPIE-sponsored conferences. The proceedings of the 1996 conference is Ref. 192. Other conferences that routinely include papers in this topic area include the annual International Conference on Plasma Science, the annual meetings of the Division of Plasma Physics, American Physical Society, the biennial Microwave Power Tube Conference, and the biennial International Conference on High-Power Particle Beams.

Gyrotron research and development is an important focus of the annual International Conference on Infrared and Millimeter Waves; its Conference Digest contains brief versions of the research papers, and many of these are subsequently published in the International Journal of Infrared Millimeter Waves. The 21st conference in this series was held in Berlin, Germany in July 1996 (see Ref. 193), and the 22nd was held in Wintergreen, VA in July 1997 (see Ref.

194). Gyrotron oscillator research and development was also the subject of a recent book (see Ref. 195). FEL research, both at short and long wavelengths, is the focus of a series of annual International Free-Electron Laser Conferences. The eighteenth in this series was held in Rome, Italy in August 1996, and the nineteenth was held in Peking, China in August 1997. The proceedings of the 1995 conference is Ref. 196. The development of rf sources for high-energy electron-positron colliders is also the subject of a series of workshops. The proceedings of the second workshop on Pulsed rf Sources for Linear Colliders (RF94), which took place in Montauk, NY in October 1994, is Ref. 197. The Proceedings of the Third Workshop on Pulsed rf Sources for Linear Colliders (RF96), which took place in Tsukuba, Japan in April 1996, is Ref. 198.

ACKNOWLEDGMENTS

The authors are grateful to the many colleagues who have offered critical comments on portions of this article, including J. Benford, A. Fisher, A. W. Fliflet, B. Hafizi, I. Haber, W. M. Manheimer, O. A. Nezhevenko, M. I. Petelin, and J. Swegle. We are also grateful to the sponsors of our own research on microwave generation. This work was supported by the Office of Naval Research, by the Department of Energy, and by the Air Force Office of Scientific Research (in the framework of the Multidisciplinary University Research Initiative Program).

[1] G. S. Nusinovich, T. M. Antonsen, Jr., V. L. Bratman, and N. S. Ginzburg, in *Applications of High-Power Microwaves*, edited by A. V. Gaponov-Grekhov and V. L. Granatstein (Artech House, Boston, 1994), Chap. 2.
[2] L. Schächter, *Beam-Wave Interaction in Periodic and Quasi-Periodic Structures* (Springer, Berlin, 1997), Chap. 5.
[3] See, F. F. Chen, *Introduction to Plasma Physics* (Plenum, New York, 1974), Sec. 7.5.1.
[4] S. D. Korovin *et al.*, Pis'ma Zh. Tekh. Fiz. **20**, 12 (1994) [Tech. Phys. Lett. **20**, 5 (1994)].
[5] W. D. Kilpatrick, Rev. Sci. Instrum. **28**, 824 (1957).
[6] A. E. Vlieks *et al.*, *Thirteenth International Symposium on Discharges and Electrical Insulation in Vacuum*, edited by J. M. Buzzi and A. Septier (Les Éditions de Physique, Les Ulis, France, 1988), Vol. 2, p. 474.
[7] P. B. Wilson, SLAC-PUB-3674 (1985); see also, V. L. Granatstein and A. Mondelli, in *The Physics of Particle Accelerators*, AIP Conference Proceedings No. 153 (American Institute of Physics, New York, 1987), p. 1506.
[8] A. S. Gilmour, Jr., *Microwave Tubes* (Artech, Norwood, MA, 1986).
[9] K. R. Eppley, W. B. Herrmannsfeld, and R. H. Miller, in *Proceedings of the 1987 Particle Accelerator Conference*, edited by E. R. Lindstrom and L. S. Taylor (IEEE, Piscataway, NJ, 1987), p. 1809.
[10] E. A. Gelvich *et al.*, IEEE Trans. Microwave Theory Tech. **41**, 15 (1993).
[11] M. Friedman and V. Serlin, Rev. Sci. Instrum. **55**, 1074 (1984); M. Friedman *et al.*, *ibid.* **61**, 171 (1990).
[12] M. Friedman *et al.*, J. Appl. Phys. **56**, 2459 (1984).
[13] M. Friedman, Phys. Rev. Lett. **32**, 92 (1974); Appl. Phys. Lett. **26**, 366 (1975).
[14] G. I. Budker *et al.*, Part. Accel. **10**, 41 (1979).
[15] O. A. Nezhevenko, IEEE Trans. Plasma Sci. **22**, 765 (1994).
[16] V. Ya. Davydovskij, Zh. Eksp. Teor. Fiz. **43**, 886 (1962) [Sov. Phys. JETP **16**, 629 (1963)]; A. A. Kolomenskii and A. N. Lebedev, Dok. Akad. Nauk SSSR **145**, 1259 (1962) [Sov. Phys. Dokl. **7**, 745 (1963)]; C. S. Roberts and S. J. Buchsbaum, Phys. Rev. A **135**, 381 (1964).
[17] M. I. Petelin, Izv. Vyssh. Uchebn. Zaved. Radiofiz. **17**, 902 (1974) [Radiophys. Quantum Electron. **17**, 685 (1974)]; V. L. Bratman *et al.*, Int. J. Electron. **51**, 541 (1981).
[18] V. A. Flyagin *et al.*, IEEE Trans. Microwave Theory Tech. **25**, 514 (1977); J. L. Hirshfield and V. L. Granatstein, *ibid.* **25**, 522 (1977).
[19] P. Sprangle and A. Drobot, IEEE Trans. Microwave Theory Tech. **MTT-25**, 528 (1977).
[20] N. M. Kroll, P. L. Morton, and M. N. Rosenbluth, IEEE J. Quantum Electron. **QE-17**, 1436 (1981); P. Sprangle, C. M. Tang, and W. M. Manheimer, Phys. Rev. A **21**, 302 (1980).
[21] N. S. Ginzburg, Izv. Vyssh. Uchebn. Zaved. Radiofiz. **30**, 1181 (1987) [Sov. Radiophys. **30**, 865 (1987)]; G. S. Nusinovich, Phys. Fluids B **4**, 1989 (1992).
[22] V. L. Ginzburg, Izv. Akad. Nauk SSSR, Ser. Fiz. **11**, 165 (1947) (in Russian).
[23] R. B. Miller, *An Introduction to the Physics of Intense Charged Particle Beams* (Plenum, New York, 1982), Chap. 3.
[24] H. A. Davis *et al.*, IEEE Trans. Plasma Sci. **16**, 192 (1988).
[25] H. Barkhausen and K. Kurz, Phys. Z. **21**, 1 (1920) (in German).
[26] L. D. Moreland *et al.*, IEEE Trans. Plasma Sci. **22**, 554 (1994).
[27] *Megagauss Magnetic Field Generation and Pulsed Power Applications*, edited by M. Cowan and R. B. Spielman (Nova Science, Commack, NY, 1994).
[28] B. A. Baryshev *et al.*, Nucl. Instrum. Methods Phys. Res. A **340**, 241 (1994).
[29] P. T. Kirstein, G. S. Kino, and W. E. Waters, *Space-Charge Flow* (McGraw-Hill, New York, 1967), Chap. IV.
[30] P. M. Lapostolle, IEEE Trans. Nucl. Sci. **NS-24**, 1101 (1971).
[31] J. D. Lawson, *The Physics of Charged-Particle Beams* (Clarendon, Oxford, 1978), Chap. 4.
[32] M. Reiser, *Theory and Design of Charged Particle Beams* (Wiley, New York, 1994), Chaps. 3 and 6.
[33] S. Penner, in *Proceedings of the 1987 Particle Accelerator Conference*, edited by E. R. Lindstrom and L. S. Taylor (IEEE, Piscataway, NJ, 1987), p. 183.
[34] J. M. Baird and W. Lawson, Int. J. Electron. **61**, 953 (1986).
[35] J. W. Gewartowski and H. A. Watson, *Principles of Electron Tubes* (Van Nostrand, New York, 1965), Chap. 2.
[36] H. R. Jory and A. W. Trivelpiece, J. Appl. Phys. **40**, 3924 (1969).
[37] J. D. Lawson, *The Physics of Charged-Particle Beams* (Clarendon, Oxford, 1978), Chap. 3.
[38] A. S. Gilmour, Jr., *Principles of Traveling Wave Tubes* (Artech, Boston, 1994), Chaps. 5 and 6.
[39] R. True, in *Handbook of Microwave Technology*, edited by T. K. Ishii (Academic, San Diego, 1995), Vol. I, Chap. 14.
[40] S. Iannazzo, Solid-State Electron. **36**, 301 (1993).
[41] H. Riege, Nucl. Instrum. Methods Phys. Res. A **340**, 80 (1994).
[42] D. Price, J. S. Levine, and J. Benford, in SPIE Proceedings Vol. 3158 (SPIE—The International Society for Optical Engineering, Bellingham, WA, 1997), in press.
[43] M. Friedman *et al.*, Phys. Rev. Lett. **75**, 1214 (1995).
[44] J. Benford and G. Benford, IEEE Trans. Plasma Sci. **25**, 311 (1997).
[45] R. J. Barker and F. J. Agee, in SPIE Proceedings Vol. 2557 (SPIE—The International Society for Optical Engineering, Bellingham, WA, 1995), p. 300.
[46] M. Makowski, IEEE Trans. Plasma Sci. **24**, 1023 (1996).
[47] T. Nagashima *et al.*, in *Strong Microwaves in Plasmas*, edited by A. Litvak (Institute of Applied Physics, Nizhny Novgorod, 1991), Vol. 2, p. 739.
[48] G. Mourier, in *Strong Microwaves in Plasmas*, edited by A. Litvak (Institute of Applied Physics, Nizhny Novgorod, 1991), Vol. 2, p. 751.
[49] V. A. Flyagin and G. S. Nusinovich, Proc. IEEE **76**, 644 (1988).
[50] V. E. Myasnikov *et al.*, Third International Workshop on Strong Microwaves in Plasmas, Nizhny Novgorod, Russia, Aug. 1996, Abstracts, S-31.
[51] GYCOM press release, 30 May 1997.
[52] V. E. Myasnikov *et al.*, in *Conference Digest—22nd International Conference on Infrared and Millimeter Waves*, edited by H. P. Freund (available from R. H. Jackson, Code 6840 Naval Research Laboratory, Washington, DC), p. 102.
[53] K. Felch *et al.*, IEEE Trans. Plasma Sci. **24**, 558 (1996).
[54] K. Sakamoto *et al.*, Conference Proceedings—21st International Conference on Infrared and Millimeter Waves, Berlin, Germany, July, 1996, Paper AT1.
[55] K. Sakamoto *et al.*, Phys. Rev. Lett. **73**, 3532 (1994).
[56] S. Alberti *et al.*, Conference Proceedings—21st International Conference on Infrared and Millimeter Waves, Berlin, Germany, July, 1996, Paper AF1.
[57] A. W. Fliflet, *et al.*, J. Fusion Energy **9**, 31 (1990).

[58] *Applications of High-Power Microwaves*, edited by A. V. Gaponov-Grekhov and V. L. Granatstein (Artech, Boston, 1994).
[59] G. G. Denisov *et al.*, Int. J. Electron. **72**, 1079 (1992).
[60] G. Caryotakis, IEEE Trans. Plasma Sci. **22**, 683 (1994).
[61] International Linear Collider Technical Review Report 1995, SLAC-R-95-471 (Stanford Linear Accelerator Center, Stanford, CA).
[62] P. B. Wilson, in *Proceedings of the Third Workshop on Pulsed RF Sources for Linear Colliders (RF 96)*, edited by S. Fukuda [High Energy Accelerator Research Organization (KEK), Tsukuba, Japan, 1997], p. 9, and SLAC-PUB-7449 (1997).
[63] D. Sprehn, G. Caryotakis, and R. M. Phillips, in *Proceedings of the Third Workshop on Pulsed RF Sources for Linear Colliders (RF 96)*, edited by S. Fukuda [High Energy Accelerator Research Organization (KEK), Tsukuba, Japan, 1997], p. 91, and SLAC-PUB-7232, 1996.
[64] C. Bearzatto and G. Faillon, in *Proceedings of the Third Workshop on Pulsed RF Sources for Linear Colliders (RF 96)*, edited by S. Fukuda [High Energy Accelerator Research Organization (KEK), Tsukuba, Japan, 1997], p. 116.
[65] E. Wright *et al.*, in *Pulsed rf Sources for Linear Colliders*, edited by R. C. Fernow (American Institute of Physics, New York, 1995), p. 58.
[66] P. B. Wilson, presented at the 18th International Linac Conference (Linac 96), Geneva, Switzerland, August 1996 (SLAC-PUB-7263); D. Sprehn (private communication).
[67] J. Haimson *et al.*, in *Pulsed rf Sources for Linear Colliders*, edited by R. C. Fernow (American Institute of Physics, New York, 1995), p. 146.
[68] H. Mizuno, in *Proceedings of the Third Workshop on Pulsed RF Sources for Linear Colliders (RF 96)*, edited by S. Fukuda [High Energy Accelerator Research Organization (KEK), Tsukuba, Japan, 1997], p. 19.
[69] V. E. Balakin *et al.*, in *Proceedings of the Third Workshop on Pulsed RF Sources for Linear Colliders (RF 96)*, edited by S. Fukuda (High Energy Accelerator Research Organization (KEK), Tsukuba, Japan, 1997), p. 110.
[70] G. V. Dolbilov *et al.*, in *Proceedings of the Third Workshop on Pulsed RF Sources for Linear Colliders (RF 96)*, edited by S. Fukuda (High Energy Accelerator Research Organization (KEK), Tsukuba, Japan, 1997), p. 100.
[71] M. J. Smith and G. Phillips, *Power Klystrons Today* (Wiley, New York, 1995).
[72] A. M. Sessler, in *Laser Acceleration of Particles*, AIP Conference Proceedings 91, edited by P. J. Channell (American Institute of Physics, New York, 1982), p. 154.
[73] J. Haimson and B. Mecklenburg, in *Proceedings of the 1989 IEEE Particle Accelerator Conference*, edited by F. Bennett and J. Kopta (IEEE, New York, 1989), p. 243.
[74] G. A. Westenskow and T. L. Houck, IEEE Trans. Plasma Sci. **22**, 750 (1994); T. Houck and G. Westenskow, in *Pulsed rf Sources for Linear Colliders*, edited by R. C. Fernow (American Institute of Physics, New York, 1995), p. 226.
[75] T. L. Houck *et al.*, in *Proceedings of the 1995 Particle Accelerator Conference* (IEEE, Piscataway, NJ, 1995), Vol. 3, p. 1524.
[76] I. Wilson, CLIC Test Beam Facilities—Status and Results, CERN-PS-96-033 (1996).
[77] V. L. Granatstein and W. Lawson, IEEE Trans. Plasma Sci. **24**, 648 (1996).
[78] W. Lawson *et al.*, IEEE Trans. Plasma Sci. **20**, 216 (1992); S. G. Tantawi *et al.*, *ibid.* **20**, 205 (1992).
[79] H. W. Matthews *et al.*, IEEE Trans. Plasma Sci. **22**, 825 (1994).
[80] G. S. Nusinovich and H. Li, Phys. Fluids B **4**, 1058 (1992).
[81] P. E. Latham *et al.*, Phys. Rev. Lett. **72**, 3730 (1994).
[82] G. S. Nusinovich, Phys. Fluids B **4**, 1989 (1992).
[83] G. P. Saraph *et al.*, IEEE Trans. Plasma Sci. **24**, 671 (1996).
[84] V. L. Granatstein *et al.*, in *Advanced Accelerator Concepts*, AIP Conference Proceedings 398, edited by S. Chattopadhyay, J. McCullough, and P. Dahl (American Institute of Physics, New York, 1997), p. 874.
[85] M. M. Karliner *et al.*, Nucl. Instrum. Methods Phys. Res. A **269**, 459 (1988).
[86] E. V. Kozyrev *et al.*, Part. Accel. **52**, 55 (1996); E. V. Kozyrev *et al.*, in Proceedings of the 1997 Particle Accelerator Conference (in press).
[87] S. H. Gold *et al.*, IEEE Trans. Plasma Sci. **24**, 947 (1996).
[88] S. H. Gold *et al.*, Phys. Plasmas **4**, 1900 (1997).
[89] A. W. Fliflet and S. H. Gold, IEEE Trans. Plasma Sci. **24**, 957 (1996).
[90] O. A. Nezhevenko *et al.*, in Proceedings of the 1997 Particle Accelerator Conference (in press).
[91] R. A. Alvarez, Rev. Sci. Instrum. **57**, 2481 (1986).
[92] R. A. Alvarez *et al.*, IEEE Trans. Magn. **MAG-17**, 935 (1981).
[93] Z. D. Farkas, IEEE Trans. Microwave Theory Tech. **MTT-34**, 1036 (1986).
[94] P. B. Wilson, in *Applications of High-Power Microwaves*, edited by A. V. Gaponov-Grekhov and V. L. Granatstein (Artech, Boston, 1994), Chap. 7.
[95] I. Syrachev *et al.*, *Proceedings of the International Conference Linac 1994*, edited by K. Takata, Y. Yamazaki, and K. Nakahara (National Laboratory for High Energy Physics, Tsukuba, Japan, 1994), p. 475.
[96] M. I. Petelin, A. L. Vikharev, and J. L. Hirshfield, in *Advanced Accelerator Concepts*, AIP Conference Proceedings 398, edited by S. Chattopadhyay, J. McCullough, and P. Dahl (American Institute of Physics, New York, 1997), p. 822.
[97] W. M. Manheimer, G. Mesyats, and M. I. Petelin, in *Applications of High-Power Microwaves*, edited by A. V. Gaponov-Grekhov and V. L. Granatstein (Artech, Boston, 1994), Chap. 5.
[98] M. L. Osipov, Radiotekh. **1995**, 3 [Telecommun. Radio Eng. **49**, 42 (1995)].
[99] L. J. Cutrona, in *Radar Handbook*, edited by M. Skolnik (McGraw-Hill, New York, 1970), Chap. 23.
[100] V. I. Belousov *et al.*, Pis'ma Zh. Tekh. Fiz. **4**, 1443 (1978) [Sov. Tech. Phys. Lett. **4**, 584 (1978)].
[101] B. V. Bunkin *et al.*, Zh. Tekh. Fiz. Lett. **18**, 61 (1992) [Sov. Tech. Phys. Lett. **18**, 299 (1992)].
[102] D. Clunie *et al.*, in *Strong Microwaves in Plasmas*, edited by A. G. Litvak (Institute of Applied Physics, Nizhny Novgorod, 1996), Vol. 2, p. 886.
[103] J. M. Mead *et al.*, Proc. IEEE **82**, 1891 (1994).
[104] W. M. Manheimer, in *Plasma Science and the Environment*, edited by W. Manheimer, L. E. Sugiyama, and T. H. Stix (American Institute of Physics, New York, 1996), Chap. 4.
[105] G. Zorpette, IEEE Spectr. **30**, 21 (1993).
[106] R. L'Hermitte, J. Atmos. Oceanic Tech. **4**, 36 (1987).
[107] Yu. V. Bykov *et al.*, Izv. Vyssh. Uchebn. Zaved. Radiofiz. **36**, 942 (1993) [Radiophys. Quantum Electron. **36**, 723 (1993)]; Izv. Akad. Nauk. SSSR, Fiz. Atmos. Okeana **32**, 84 (1996) [Atmos. Oceanic Phys. (in press)].
[108] I. I. Antakov *et al.*, in *Strong Microwaves in Plasmas*, edited by A. G. Litvak (Institute of Applied Physics, Nizhny Novgorod, 1994), Vol. 2, p. 587.
[109] I. I. Antakov, E. V. Zasypkin, and E. V. Sokolov, Proc. SPIE **2104**, 466 (1993).
[110] M. Blank *et al.*, in *Conference Digest—22nd International Conference on Infrared and Millimeter Waves*, edited by H. P. Freund (available from R. H. Jackson, Code 6840, Naval Research Laboratory, Washington, DC, 1997), p. 224.
[111] V. P. Botavin *et al.*, International 1992 Geneva Conference on Systems and Signals, Geneva, Switzerland, June 1992, p. 51.
[112] J. J. Choi *et al.*, Bull. Am. Phys. Soc. **38**, 2000 (1993).
[113] K. R. Chu *et al.*, Phys. Rev. Lett. **74**, 1103 (1995).
[114] K. R. Chu, in *Conference Digest–22nd International Conference on Infrared and Millimeter Waves*, edited by H. P. Freund (available from R. H. Jackson, Code 6840, Naval Research Laboratory, Washington, DC, 1997), paper Th4.1.
[115] Q. S. Wang *et al.*, IEEE Trans. Plasma Sci. **24**, 700 (1996).
[116] R. A. Mahaffey *et al.*, Phys. Rev. Lett. **39**, 843 (1977).
[117] D. J. Sullivan, IEEE Trans. Nucl. Sci. **NS-30**, 3426 (1983).
[118] L. E. Thode, in *High Power Microwave Sources*, edited by V. L. Granatstein and I. Alexeff (Artech, Boston, 1987), Chap. 14.
[119] J. Benford and J. Swegle, *High Power Microwaves* (Artech, Boston, 1992), Chap. 9.
[120] H. A. Davis *et al.*, IEEE Trans. Plasma Sci. **18**, 611 (1990).
[121] C.-S. Hwang and M.-W. Wu, IEEE Trans. Plasma Sci. **21**, 239 (1993).
[122] H. Sze *et al.*, J. Appl. Phys. **68**, 3073 (1990).
[123] E. I. Azarkevich *et al.*, Teplofiz. Vys. Temp. **32**, 127 (1994) [High Temp. (USSR) **32**, 122 (1994)].
[124] G. A. Huttlin *et al.*, IEEE Trans. Plasma Sci. **18**, 618 (1990).
[125] J. W. Gewartowski and H. A. Watson, *Principles of Electron Tubes* (Van Nostrand, New York, 1965), Chap. 9.
[126] M. Friedman and V. Serlin, Phys. Rev. Lett. **55**, 2860 (1985); M. Friedman *et al.*, Rev. Sci. Instrum. **61**, 171 (1990).
[127] M. Friedman *et al.*, Phys. Rev. Lett. **75**, 1214 (1995).
[128] M. Friedman *et al.*, in SPIE Proceedings Vol. 1407 (SPIE—The international Society for Optical Engineering, Bellingham, WA, 1991), p. 2; M. Friedman and V. Serlin, in SPIE Proceedings Vol. 1629 (SPIE—The International Society for Optical Engineering, Bellingham, WA, 1992), p.

2; M. Friedman *et al.*, in SPIE Proceedings Vol. 2154 (SPIE—The International Society for Optical Engineering, Bellingham, WA, 1994), p. 2.
[129] M. Friedman, J. Appl. Phys. **80**, 1263 (1996); M. Friedman (private communication).
[130] K. J. Hendricks *et al.*, Phys. Rev. Lett. **76**, 154 (1996).
[131] J. S. Levine and B. D. Harteneck, Appl. Phys. Lett. **65**, 2133 (1994).
[132] M. V. Fazio *et al.*, IEEE Trans. Plasma Sci. **22**, 740 (1994).
[133] R. B. Miller *et al.*, IEEE Trans. Plasma Sci. **22**, 701 (1994); Proc. SPIE **2557**, 2 (1995).
[134] J. Nation, Appl. Phys. Lett. **17**, 491 (1970).
[135] N. F. Kovalev *et al.*, Pis'ma Zh. Tekh. Fiz. **18**, 232 (1973) [JETP Lett. **18**, 138 (1973)].
[136] Y. Carmel *et al.*, Phys. Rev. Lett. **33**, 1278 (1974).
[137] E. B. Abubakirov *et al.*, Pis'ma Zh. Tekh. Fiz. **9**, 533 (1983) [Sov. Tech. Phys. Lett. **9**, 230 (1983)].
[138] N. F. Kovalev and V. I. Petrukhina, Elektron. Tekh., Ser. 1, ESVCh **1977**, 102 (in Russian).
[139] S. D. Korovin, V. V. Rostov, and A. V. Smorgonskii, Izv. Vyssh. Uchebn. Zaved. Radiofiz. **29**, 1278 (1986) (in Russian).
[140] S. D. Korovin *et al.*, Pis'ma Zh. Tekh. Fiz. **18**, 63 (1992) [Sov. Tech. Phys. Lett. **18**, 265 (1992)].
[141] E. B. Abubakirov *et al.*, Zh. Tekh. Fiz. **60**, 186 (1990) [Sov. Phys. Tech. Phys. **35**, 1341 (1990)].
[142] D. Shiffler *et al.*, J. Appl. Phys. **70**, 106 (1991).
[143] L. Schächter *et al.*, in *Pulsed rf Sources for Linear Colliders*, edited by R. C. Fernow (American Institute of Physics, New York, 1995), p. 162.
[144] S. P. Bugaev *et al.*, IEEE Trans. Plasma Sci. **18**, 525 (1990); **18**, 518 (1990).
[145] M. V. Kuzelev *et al.*, Fiz. Plazmy **13**, 1370 (1987) [Sov. J. Plasma Phys. **13**, 793 (1987)].
[146] V. I. Krementsov *et al.*, Zh. Eksp. Teor. Fiz. **75**, 2151 (1978) [Sov. Phys. JETP **48**, 1084 (1978)].
[147] Y. Carmel *et al.*, Phys. Rev. Lett. **62**, 2389 (1989); Phys. Fluids B **4**, 2286 (1992).
[148] M. V. Kuzelev *et al.*, Zh. Eksp. Teor. Fiz. **109**, 2048 (1996) [JETP **82**, 1102 (1996)].
[149] G. Bekefi and T. Orzechowski, Phys. Rev. Lett. **37**, 379 (1976).
[150] N. F. Kovalev *et al.*, Pis'ma Zh. Tekh. **6** 459 (1980) [Sov. Tech. Phys. Lett. Sov. Tech. Phys. Lett. **6**, 197 (1980).
[151] J. Benford *et al.*, IEEE Trans. Plasma Sci. **PS-13**, 538 (1985).
[152] J. S. Levine *et al.*, J. Appl. Phys. **70**, 2838 (1991); J. Benford *et al.*, IEEE Trans. Plasma Sci. **21**, 388 (1993).
[153] J. S. Levine *et al.*, in SPIE Proceedings Vol. 2557 (SPIE—The International Society for Optical Engineering, Bellingham, WA, 1995), p. 74.
[154] S. E. Calico *et al.*, in SPIE Proceedings Vol. 2557 (SPIE—The International Society for Optical Engineering, Bellingham, WA, 1995), p. 50.
[155] V. L. Granatstein *et al.*, Plasma Phys. **17**, 23 (1975).
[156] N. S. Ginzburg *et al.*, Zh. Tekh. Fiz. **49**, 378 (1979) [Sov. Phys. Tech. Phys. **24**, 218 (1979)].
[157] S. N. Voronkov *et al.*, Zh. Tech. Fiz. **52**, 106 (1982) [Sov. Phys. Tech. Phys. **27**, 68 (1982)]; V. V. Bogdanov *et al.*, Zh. Tekh. Fiz. **53**, 106 (1983) [Sov. Phys. Tech. Phys. **28**, 61 (1983)].
[158] S. H. Gold *et al.*, Phys. Fluids **30**, 2226 (1987); IEEE Trans. Plasma Sci. **16**, 142 (1988).
[159] W. M. Black *et al.*, Phys. Fluids B **2**, 193 (1990).
[160] M. T. Walter *et al.*, IEEE Trans. Plasma Sci. **24**, 636 (1996).
[161] T. A. Spencer *et al.*, IEEE Trans. Plasma Sci. **24**, 630 (1996).
[162] S. H. Gold *et al.*, IEEE Trans. Plasma Sci. **18**, 1021 (1990).
[163] S. H. Gold *et al.*, J. Appl. Phys. **69**, 6696 (1991).
[164] W. L. Menninger *et al.*, IEEE Trans. Plasma Sci. **24**, 687 (1996).
[165] V. L. Bratman and G. G. Denisov, Int. J. Electron. **72**, 969 (1992).
[166] A. C. DiRienzo *et al.*, Phys. Fluids B **3**, 1755 (1991).
[167] S. J. Cooke *et al.*, Phys. Rev. Lett. **77**, 4836 (1996).
[168] V. L. Bratman *et al.*, Phys. Rev. Lett. **75**, 3102 (1995).
[169] R. M. Phillips, IRE Trans. Electron Devices **ED-7**, 231 (1960).
[170] S. I. Krementsov, M. D. Raizer, and A. V. Smorgonskii, Pis'ma Zh. Tekh. Fiz. **2**, 453 (1976) [Sov. Tech. Phys. Lett. **2**, 175 (1976)].
[171] T. C. Marshall, *Free-Electron Lasers* (Macmillan, New York, 1985), Chap. 7.
[172] J. Benford and J. Swegle, *High Power Microwaves* (Artech, Boston, 1992), Chap. 7.
[173] R. K. Parker *et al.*, Phys. Rev. Lett. **48**, 238 (1982).
[174] S. H. Gold *et al.*, Phys. Fluids **27**, 746 (1984); Phys. Rev. Lett. **52**, 1218 (1984).
[175] T. J. Orzechowski *et al.*, Phys. Rev. Lett. **57**, 2172 (1986).
[176] S. L. Allen *et al.*, Phys. Rev. Lett. **72**, 1348 (1994); S. L. Allen and E. T. Scharlemann, in *Proceedings of the 9th International Conference on High-Power Particle Beams*, edited by D. Mosher and G. Cooperstein (available from the National Technical Information Service, Springfield, VA, 1992), p. 247.
[177] M. E. Conde and G. Bekefi, IEEE Trans. Plasma Sci. **20**, 240 (1992).
[178] V. L. Bratman *et al.*, IEEE Trans. Plasma Sci. **24**, 744 (1996).
[179] S. Cheng *et al.*, IEEE Trans. Plasma Sci. **24**, 750 (1996).
[180] K. Saito *et al.*, in *Proceedings of the 17th International Free Electron Laser Conference*, edited by I. Ben-Zvi and S. Krinsky (North Holland, Netherlands, 1996), p. 237.
[181] A. K. Kaminsky *et al.*, in *Proceedings of the 17th International Free Electron Laser Conference*, edited by I. Ben-Zvi and S. Krinsky (North Holland, Netherlands, 1996), p. 215.
[182] M. A. Agafonov *et al.*, in *Proceedings of the 11th International Conference on High-Power Particle Beams*, edited by K. Jungwirth and J. Ullschmied (Academy of Sciences of the Czech Republic, Prague, 1996), Vol. I, p. 213.
[183] Yu. V. Bykov and V. E. Semenov, in *Applications of High-Power Microwaves*, edited by A. V. Gaponov-Grekhov and V. L. Granatstein (Artech, Boston, 1994), Chap. 8.
[184] J. N. Benford, in *Applications of High-Power Microwaves*, edited by A. V. Gapanov-Grekhov and V. L. Granatstein (Artech, Boston, 1994), Chap. 6.
[185] G. S. Nusinovich, G. M. Milikh, and B. Levush, J. Appl. Phys. **80**, 4189 (1996).
[186] R. Heidinger *et al.*, in *Conference Digest—22nd International Conference on Infrared and Millimeter Waves*, edited by H. P. Freund (available from R. H. Jackson, Code 6840, Naval Research Laboratory, Washington, DC., 1997), p. 142.
[187] O. Braz *et al.*, *ibid.*, p. 144.
[188] *High Power Microwave Sources*, edited by V. L. Granatstein and I. Alexeff (Artech, Boston, 1987).
[189] J. Benford and J. Swegle, *High Power Microwaves* (Artech House, Boston, 1992).
[190] C. D. Taylor and D. V. Giri, *High-Power Microwave Systems and Effects* (Taylor and Francis, Washington, DC, 1994).
[191] Sixth Special Issue on High-Power Microwave Generation, edited by G. S. Nusinovich and K. Kreischer, IEEE Trans. Plasma Sci. **24**, 552 (12996).
[192] *Intense Microwave Pulses IV*, SPIE Proceedings Vol. 2843, edited by H. E. Brandt (SPIE—The International Society for Optical Engineering, Bellingham, WA, 1996).
[193] *Conference Proceeding—21st International Conference on Infrared and Millimeter Waves*, edited by M. von Ortenberg and H.-U. Mueller (Humboldt Universität zu Berlin, Berlin, Germany, 1996).
[194] *Conference Digest—22nd International Conference on Infrared and Millimeter Waves*, edited by H. P. Freund (available from R. H. Jackson, Code 6840, Naval Research Laboratory, Washington, DC, 1997).
[195] *Gyrotron Oscillators—Their Principles and Practice*, edited by C. J. Edgcombe (Taylor and Francis, London, 1993).
[196] *Proceedings of the Seventeenth International Free Electron Laser Conference*, edited by I. Ben-Zvi and S. Krinsky (North Holland, Netherlands, 1996).
[197] *Pulsed rf Sources for Linear Colliders*, AIP Conference Proceedings 337, edited by R. C. Fernow (American Institute of Physics, New York, 1995).
[198] *Proceedings of the Third Workshop on Pulsed RF Sources for Linear Colliders (RF 96)*, edited by S. Fukuda [High Energy Accelerator Research Organization (KEK), Tsukuba, Japan, 1997].